AD_____

Award Number: W81XWH-12-1-0115

TITLE:

Systematic Characterization of the Molecular Mechanisms That Regulate and Mediate Alternative Lengthening of Telomeres in Breast Carcinoma

PRINCIPAL INVESTIGATOR: Yaara Zwang

CONTRACTING ORGANIZATION:

Dana-Farber Cancer Institute
450 Brookline Ave
Boston, MA 02115-6013

REPORT DATE: June 2015

Type of Report: Annual Summary

PREPARED FOR: U.S. Army Medical Research and Materiel Command
Fort Detrick, Maryland 21702-5012

DISTRIBUTION STATEMENT: Approved for Public Release;
Distribution Unlimited

The views, opinions and/or findings contained in this report are those of the author(s) and should not be construed as an official Department of the Army position, policy or decision unless so designated by other documentation.

REPORT DOCUMENTATION PAGE

Form Approved
OMB No. 0704-0188

Public reporting burden for this collection of information is estimated to average 1 hour per response, including the time for reviewing instructions, searching existing data sources, gathering and maintaining the data needed, and completing and reviewing this collection of information. Send comments regarding this burden estimate or any other aspect of this collection of information, including suggestions for reducing this burden to Department of Defense, Washington Headquarters Services, Directorate for Information Operations and Reports (0704-0188), 1215 Jefferson Davis Highway, Suite 1204, Arlington, VA 22202-4302. Respondents should be aware that notwithstanding any other provision of law, no person shall be subject to any penalty for failing to comply with a collection of information if it does not display a currently valid OMB control number. **PLEASE DO NOT RETURN YOUR FORM TO THE ABOVE ADDRESS.**

1. REPORT DATE	**2. REPORT TYPE**	**3. DATES COVERED**
June 2015	Annual Summary	15 Mar 2012 - 14 Mar 2015

4.
TITLE AND SUBTITLE: Systematic Characterization of the Molecular Mechanisms That Regulate and Mediate Alternative Lengthening of Telomeres in Breast Carcinoma

5a. CONTRACT NUMBER

5b. GRANT NUMBER
W81XWH-12-1-0115

5c. PROGRAM ELEMENT NUMBER

6. AUTHOR(S) Yaara Zwang

E-Mail: yaarac_zwang@dfci.harvard.edu

5d. PROJECT NUMBER

5e. TASK NUMBER

5f. WORK UNIT NUMBER

7. PERFORMING ORGANIZATION NAME(S) AND ADDRESS(ES)

Dana-Farber Cancer Institute
450 Brookline Ave
Boston, MA 02115-6013

8. PERFORMING ORGANIZATION REPORT NUMBER

9. SPONSORING / MONITORING AGENCY NAME(S) AND ADDRESS(ES)
U.S. Army Medical Research and Materiel Command
Fort Detrick, Maryland 21702-5012

10. SPONSOR/MONITOR'S ACRONYM(S)

11. SPONSOR/MONITOR'S REPORT NUMBER(S)

12. DISTRIBUTION / AVAILABILITY STATEMENT
Approved for Public Release; Distribution Unlimited

13. SUPPLEMENTARY NOTES

14. ABSTRACT

Alternative lengthening of telomeres (ALT) is a mechanism utilized by several cancer types to maintain telomeres. The aim of this project is to characterize the mechanisms that mediate and regulate ALT activity in breast cancer, by utilizing proteomic and genomic approaches to describe and perturb ALT+ cells. Gaining this knowledge on ALT activity can promote the development of novel treatment for ALT+ breast tumors, and patients with telomerase inhibitor resistant tumors, while having minimal non-desired effects on the normal cell population that typically has no ALT activity. Here, I report on my progress in profiling and analyzing a collection of ALT+ and non-ALT cell-lines in order to define an ALT+ expression signature, which highlights potential mechanism and vulnerabilities of ALT+ cells. In addition, I report on the profiling of transcriptional changes that occur upon suppression of ATRX.

15. SUBJECT TERMS					
Nothing listed					
16. SECURITY CLASSIFICATION OF:			17. LIMITATION OF ABSTRACT	18. NUMBER OF PAGES	19a. NAME OF RESPONSIBLE PERSON USAMRMC
a. REPORT U	b. ABSTRACT U	c. THIS PAGE U	UU	55	19b. TELEPHONE NUMBER *(include area code)*

Clarification regarding this year progress

My efforts were focused on two main sub-aims during that year: 1. studying the transcriptional events that occur in cells upon ATRX suppression, and analysis of the ALT+ gene signature that I generated. This effort is designed to achieve the goals of Task 2 as it appears in the SOW. 2. Searching for positive controls for suppression of ALT activity. This effort is relevant for Tasks 1 and 3.

Studying ALT-specific transcriptome

I analyzed the two gene expression datasets described in the report to generate two gene signatures. I used these signatures to identify pathways and modules that are involved in ALT activity in an attempt to identify potential targets in ALT-positive cancers and in order to achieve better understanding of the cellular status associated with ALT activity. A major finding of these analyses is that HER2 inhibition as well as CDK2, and HDAC inhibition can reverse the ALT+ gene signature. This finding has a therapeutic potential and I am in the process of validating it and characterizing it in order to confirm its relevance. Similarly, a gene-set enrichment analysis identified an enrichment of DNA repair related genes in ALT+ cells. Since ALT activity is likely to increase the burden of DNA repair requirement in the cells, it is possible that the increased expression of DNA repair genes is essential for the survival of ALT+ cells, and is therefore a potential target. The outcome of suppressing DNA repair mechanism in ALT+ cells is among the questions I am studying now.

This research was included in the report.

Searching for positive controls for suppression of ALT activity

In parallel to the analysis of the gene expression data, I am also putting an effort toward identifying new positive controls for Task 3. As was included in the SOW and in previous reports, I tried to use genes that are known to be involved in ALT activity as positive controls for Task 3. I obtained multiple shRNAs for each of the genes, however, as shown in Figure 1 of the report, I could not achieve a dynamic range that is sufficient for an HTS screen. Therefore, I am attempting to identify better positive controls for ALT activity suppression. Part of this search uses the gene expression data that I generated in Task 2 to guide the selection of new potential positive controls by testing genes whose expression in ALT+ cells is significantly higher than in non-ALT cells. Identifying robust positive controls with a wide dynamic range

is essential for the success of Task 3, since it will determine the threshold of calling genes as hits in the screen, and is therefore will determine the specificity (false positive rate) and sensitivity (false negative rate) of the screen. Importantly, the genes that were planned to be used as positive controls in Task 3 are also the genes that I planned to use to suppress ALT activity for Task 1. According to the C-circle assay, the suppression of these genes resulted in only partial suppression of ALT activity. In order to reliably identify proteins associated with PML and Sp100 in ALT+ cells by mass-spectrometry analysis, it is essential to achieve a strong suppression of ALT activity in the perturbed samples. As described above, I am using the gene expression data to search for genes whose perturbation leads to stronger suppression of ALT activity. I expect to proceed with both Task 1 and Task 3 as planned as soon as I resolve this issue.

In addition, as I have shown in previous reports, I adjusted the C-circle assay to allow quantitative and more sensitive detection of C-circle abundance. However, the throughput of the assay was not optimal for a screening experiment. I am working on further improving the assay and adjusting it for higher throughput experiments. The main strategy is to enable detection of C-circles by qPCR rather than by probe hybridization. This optimization of the assay used as a readout in a HTS screen as planned in Task 3 is important for the success of the screen, and therefore I am investing in it.

This clarification regarding Task 1 and 3 was added to the revised report.

TYPE OF REPORT: Final-Addendum

PREPARED FOR: U.S. Army Medical Research and Materiel Command

Fort Detrick, Maryland 21702-5012

DISTRIBUTION STATEMENT: Approved for Public Release;

Distribution Unlimited

The views, opinions and/or findings contained in this report are those of the author(s) and should not be construed as an official Department of the Army position, policy or decision unless so designated by other documentation.

Table of Contents

Introduction

The capacity to maintain elongated telomeres is an essential feature of tumor cells enabling their unlimited replicative potential. Approximately 85-90% of human cancers maintain telomeres through activation of telomerase. However, several cancer types harness telomerase-independent mechanisms referred to as Alternative Lengthening of Telomeres (ALT). Importantly, inhibition of telomerase in immortalized premalignant cells and in cancer cells induces a switch from telomerase activation to ALT, enabling the cells to escape therapy (*1*, *2*).

The phenotypic characteristics of ALT+ cells include long and heterogeneous telomeric DNA, ALT-associated PML Bodies (APBs), high level of recombination at telomeres, and abundant extrachromosomal telomeric DNA, especially single strand C-rich circles (C-circles)(*3*). Currently, there is limited molecular understanding of the mechanisms that induce ALT and that are involved in ALT activity.

Importantly, ALT activity has been reported in breast carcinomas, where it was correlated with HER2 positivity and with poor prognosis (*4*). Furthermore, a recent report showed that ALT activity and hTERT expression can co-exist in the same cells in patient breast tumor smaples (*5*). Hence, understanding the mechanisms that regulate and facilitate ALT activity can promote the development of novel treatments for telomerase-independent breast cancer. Such treatment has an attractive potential in helping patients with ALT+-poor prognosis breast cancer and as a combination therapy for patients treated with telomerase inhibitors. It is expected that inhibition of ALT activity will have minimal non-desired effects on the normal cell population that typically has no ALT activity.

The aim of this project is to characterize the mechanisms that mediate and regulate ALT activity in breast cancer, by utilizing proteomic and genomic approaches to describe and perturb ALT+ cells.

Keywords

ALT (alternative lengthening of telomeres), immortalization, ATRX, C-circles, Gene expression profiling.

Overall project summary

Calibrating C-circle assay to allow robust quantification

In order to allow accurate quantification of C-circles abundance, the detection method was modified to enable digital acquisition of the signal with high sensitivity. Using LiCor Odessey imaging system along with Image Studio software allows automatic quantification of the dot-blot labeled with IRdye-conjugated probes. This adjustment improved the sensitivity of the assay enabling detection of C-circles in only 20ng of genomic DNA. In addition, converting to a fluorescence-labeling method allows safer processing of multiple samples at the same time.

An Alu repeat probe was used in parallel to the C-circle probe to normalize the C-circle signal to the input amount of genomic DNA, thus enabling better quantitation of ALT activity.

Testing these adjustments on ALT+ cells, known to have variable level of C-circles, demonstrated a wide range of sensitivity and very low background from non-ALT cells (Figure 1A). Additionally, I tested 4 shRNAs that target proteins known to be involved in ALT activity (*6-8*). In contrast to LacZ-specific shRNA that had no effect on C-circle abundance, targeting RAD51, MUS81, SMC5, and RAD50 reduced the C-circle signal, suggesting a reduction in ALT-related recombination activity (Figure 1B).

Therefore, the adjustments I introduced to the C-circle assay retain the sensitivity of the assay and importantly, improve quantification and assay handling.

Study ATRX and DAXX involvement in ALT

A study by Heaphy et al. (*9*) found that pancreatic neuroendocrine tumors that exhibit features of ALT activity, also have alternations in ATRX and DAXX. It was found that these tumors had either *ATRX* or *DAXX* mutations or lacked their nuclear expression at the protein level. A similar correlation between ATRX and ALT activity was also found in pediatric glioblastomas (*10*), liposarcomas (*11*). A recent report also showed that overexpression of ATRX in ALT+ fibroblasts can suppressed ALT activity (*12*). DAXX and ATRX are histone chaperones associated with replication-independent deposition of Histone H3.3 (*13, 14*). ATRX was shown to be localized at telomeres and to associate with structural maintenance of telomeres integrity (*15*). To test potential involvement of ATRX in breast cancer, we analyzed its status across the TCGA data-set for breast invasive carcinoma, and found that it is mutated in 2% of the tumors sequenced by TCGA (cBio portal analysis).

To further study ATRX involvement in ALT activation, we first tested its expression in a panel of 22 ALT+ cell-lines, showing that in 16 cell-lines ATRX expression was undetectable (Figure 1A in (*16*)). DAXX expression was reduced in only 4 of the tested ALT+ cell-lines. In 3 cell-lines that expressed ATRX protein, it did not exhibit a punctuated nuclear localization, suggesting loss of functional ATRX (Figure 1B in (*16*)).

The observed association between ALT activity and loss of functional ATRX encouraged me to test whether knock-down of ATRX or DAXX in non-immortalized cells will promote immortalization through activation of ALT. To this end, I used BJ cells stably expressing SV40-Early Region non-immortalized cell-line. Control cells, infected with shRNA targeting LacZ, did

not undergo immortalization, but rather exhibited a gradual decrease in population doubling rate, and eventually stopped proliferating at accumulated population doubling 66 (day 73), typical to these cells (Figure 2A).

To test the hypothesis that loss of ATRX or DAXX are involved in ALT-mediated immortalization, I introduced shRNAs to knock-down ATRX and DAXX in BJ cells, and the cells were passaged in culture for 110 days. Knock-down of either ATRX or DAXX did not facilitate a rapid immortalization typical to hTERT overexpression. However, after 58 and 65 days in culture, two immortal clones emerged in shATRX589- and shATRX590-infected plates, respectively. While the population doubling rate before the emergence of the two clones was similar to that of control (shLacZ1650-infected) cells, this rate significantly increased to become similar to the rate of hTERT-immortalized cells, indicating a complete recovery of population crisis (Figure 2B, compare week 7 to week 15).

Investigating the mechanism by which the emerged two colonies underwent immortalization, I found that the expression of hTERT significantly increased in the two immortalized shATRX colonies (Figure 3A). This result suggested that the mechanism of telomere maintenance in the two shATRX immortalized colonies is telomerase-mediated. To verify that ALT activity is not involved, I used the C-circle assay. In accordance with telomerase-mediated telomere maintenance, there was no evidence for activation of ALT in the two shATRX immortalized colonies (Figure 3B).

Another feature related to telomere maintenance, is the expression of TERRA (telomeric repeat-containing RNA), that are transcribed from subtelomeric and telomeric regions. TERRA are associated with telomeres forming a heterochromatin complex, which was suggested to negatively regulate telomerase activity in a telomere-length-dependent manner (*17*). In addition, in tumor cells, telomerase activity correlates with lower TERRA expression, compared to ALT-mediated telomere maintenance (*18*). Testing the expression of several TERRA transcribed from different chromosomes, showed that at early population doubling TERRA expression in control cells and shATRX-infected cells is similar (Figure 3C, left panel). However, upon immortalization, the two shATRX colonies exhibited a significantly reduced expression of TERRA (Figure 3C, right panel), in accordance with activation of functional telomerase.

To summarize, knock-down of either ATRX or DAXX did not facilitate rapid immortalization and ALT activation in cells. Lack of ATRX activity was shown before to be associated with modest level of telomere dysfunction (*15*). A recent report by Clynes et.al. also showed that ATRX suppression is not sufficient to induce ALT activity (*19*). Moreover, this report demonstrated that ATRX suppression leads to DNA damage response in telomeres. To survive, the cells are forced to activate a mechanism that elongate and maintain telomeres. This resolution is typically a rare event which occurs at a single cell allowing a significant increase in proliferation rate that eventually result in the emergence of an immortalized colony that will rapidly take-over, the otherwise arrested, population. Though the cells I used resolved this by activation of telomerase, it is nevertheless possible that under other cellular contexts, this could be resolved by activation

of ALT, as is indicated by the correlation of ALT occurrence with ATRX mutations and lack of expression.

Unbiased analysis of transcriptional profiles of ALT+ and non-ALT cells

In order to characterize the unique transcriptional profile of ALT+ cells, I measured the steady-state global transcriptional program of 16 ALT+ and 9 non-ALT cell-lines using the Affymetrix microarray HTU133A platform.

In order to visualize the variance in the data, I used Principal Component Analysis (PCA), which allows the unbiased identification of major sub-groups of cell-lines within the complete data set that exhibit higher correlation to each other. As shown in Figure 4A, the first two PCAs with the highest variance clustered the cell-lines into two major groups according to their ALT activity. Importantly, this analysis shows that the ALT+ cell-lines correlate better with each other than with non-ALT cell-lines. Furthermore, this analysis also indicates that the most significant feature that distinguishes the samples is their ALT activity, since the two most variant PCAs were able to distinguish the ALT+ from the non-ALT cell-lines.

To explore the unique transcriptional profile related to ALT activity, I first identified the genes that exhibit variability within the data using GenePattern (*20*). A total of 9,909 probes exhibited over two-fold change and a minimal delta of 50 across cell-lines (pre-normalized data), independent of ALT-activity status. In accordance with the PCA analysis (Figure 4A), a correlation matrix of all the samples showed two major clusters distinguishing cell-lines by their ALT activity (Figure 4B). The correlation coefficients presented here are affected by cell-line specific expression patterns as well as by ALT-related patterns since all the genes that exhibited variability across all samples were included in computing this correlation matrix. This suggests that the contribution of ALT-related expression patterns is significant enough to lead an unbiased clustering of the measured cell lines.

Studying the differential expression pattern of ALT+ cells

To facilitate better understanding of the molecular mechanisms that are related to ALT activity, I used the GenePattern Comparative Marker Selection module to identify genes that exhibit differential expression between ALT+ and non-ALT cell-lines (*21*). The genes were then ranked-ordered by this score (Figure 5A). Based on this analysis, I identified 5022 genes whose differential expression significantly (q-value<0.01) correlates with ALT activity, of which 2147 genes had a q-value<0.001 (corresponding to FDR<0.1%; Figure 5B).

Investigating the list of differentially expressed genes revealed that several known ALT-related genes were indeed up-regulated in ALT+ cells. Members of the MRN complex, which is essential for telomere elongation in ALT+ cell-lines (*6*), MRE11, RAD50, and XRCC1, were significantly up-regulated in ALT+ compared to non-ALT cell-lines (Figure 5C-E). Additional genes associated with ALT activity, such as SMC5/6, FEN1, ASF1B, RECQL, MUS81, TREF1/2, FANCL, and SP100, were also significantly up-regulated in the ALT+ cell-lines.

To further study the unique gene expression pattern of ALT+ cell-lines, I took an unbiased approach to analyze the gene signature identified above by using GSEA (Gene Set Enrichment Analysis) tool. First, I analyzed the enrichment of the ALT-related signature genes against all Gene Ontology (GO) gene sets. Each of the sets in this collection consists of genes that are annotated by the same GO term. 24 out of the 1025 gene sets included in this collection were significantly enriched for in the ALT+ cell-lines with a nominal p-value lower than 1%. Several of the enriched gene sets were associated with DNA replication, mitosis, chromosome segregation, and spindle regulation (Table 1). Interestingly, one of the top enriched gene sets identified here is termed 'ATP DEPENDENT DNA HELICASE ACTIVITY' (Figure 6A), which includes genes whose activity relates to the MRN complex as well as to BLM and WRN.

A second gene set collection I used consists of curated gene sets that are based on data from the literature, pathway databases (such as KEGG and REACTOM), and perturbation datasets. 153 out of the 3767 gene sets included in this collection were significantly enriched for in the ALT+ cell-lines with a nominal p-value lower than 1% (Table 2). Several of the enriched gene sets identified in this analysis are related to DNA synthesis and more specifically, to the synthesis of the lagging strand (Figure 6B). Confirming the relevance of this gene set to ALT activity, the set includes FEN1, which is essential for stabilizing telomeres in ALT+ cells but not in normal or telomerase-active cells (*22*). Additional enriched gene sets that could potentially be relevant to ALT+ cell-lines are sets related to DNA repair and maintenance of stability (Figure 6C). ALT activity involves extensive recombination at the chromosomal ends, and thus could increase the overall burden of DNA repair in the cell. Therefore, over-expression of repair genes could be essential for maintaining DNA stability in ALT+ cells. Of note, several of the genes included in the set, such as AURKA, are already being tested as targets for targeted therapy in breast cancer, suggesting ALT+ breast tumors could benefit from these drugs (*23*, *24*).

Finally, a gene set consisting of genes encoding kinases that are differentially expressed in basal breast cancer was enriched for in the ALT+ cell-lines (Figure 6D) (*25*). Most of these kinases are associated with cell-cycle regulation, such as AURKA, AURKB, BUB1, and CDK1. PLK1 was reported to contribute to ALT activity by phosphorylating TREF1, thus promoting it's binding and stabilization of telomeres (*26*). Likewise, CDK1 regulates the replication of telomeric DNA in telomerase-negative cells (*27*), and also phosphorylates TREF1 to promote its recruitment to sites of DNA damage (*28*).

The differential expression of these genes between ALT+ and non-ALT cell-lines could potentially be utilized to gain therapeutic specificity, however, further investigation of the contribution of these kinases to ALT activity is necessary.

To summarize, ALT+ cell-lines exhibit a differential expression pattern as compared to non-ALT cell-lines. This ALT-related expression signature includes several known ALT-related genes, which signifies its relevance to understanding the mechanisms that mediate and regulate ALT activity. Using statistical analysis tools, I identified several sets of genes that are differentially expressed in ALT+ cell-lines and are potentially involved in ALT activity and the survival of ALT+ cells.

Predicting sensitivity to drugs using the ALT+ gene signature

The Connectivity Map dataset contains over 6000 gene expression profiles from human cells treated with small molecule compounds (*29*). The connectivity Map tool compares a query gene signature of interest, consisting of up- and down-regulated genes, to all the gene signatures in its dataset. The connection between the query signature and each of the dataset signatures is calculated using rank-based pattern matching and scored according to Kolmogorov-Smirnov statistics.

Using the ALT+ gene expression signature generated above as a query signature, I generated a list of small molecule compounds whose gene signatures are negatively connected to the ALT+ signature (Table 3). Potentially, negatively connected compounds reverse the given query signature, suggesting that few of the identified compounds could convert the ALT+ state of gene expression into non-ALT cellular state. Interestingly, 3 of the top 20 compounds that had a strong negative connectivity to the ALT+ signature have known relevance to breast cancer; The strongest negative connection identified is the perturbation of cells with the HER2 inhibitor AG-825. This connectivity suggests that treating HER2 positive, ALT-dependent breast tumors with an HER2 inhibitor would affect the tumor cells both by inhibiting the oncogenic HER2 activity, and by reverting the ALT-specific signature. Likewise, the HDAC inhibitor MS-275 (Entinostat) and the CDK2 inhibitor GW-8510 are also negatively connected to the ALT+ gene signature. Both inhibitors have been tested in breast cancer (*30*, *31*), and potentially could have greater efficiency in ALT+ breast tumors due to their ability to revert the ALT+ cellular state.

Analysis of gene expression patterns upon ATRX knock-down

Several reports indicate the involvement of ATRX in ALT activity and in telomere maintenance. Since ATRX is a chromatin remodeler it is expected that suppression of ATRX will affect the expression of multiple genes, including genes that regulate ALT activity. Although knocking-down ATRX in BJ cells resulted in immortalization facilitated by hTERT expression rather than ALT activation (see above and (*16*)), I expected that the suppression of ATRX would still affect the expression of genes that are involved in ALT activity. Therefore, I profiled the steady-state transcriptome of both parental BJ cells and shATRX589-immortalized cells by RNAseq using Illumina HiSeq platform. Reads were aligned, mapped, and counted using the Tuxedo tools. The 10,000 highest-expressing genes were considered for further analysis of differential expression in order to ensure that signals are above noise (Figure 7A). To identify differentially expressing genes, I calculated the fold-change in expression upon shATRX-mediated immortalization. There are 745 genes that exhibit more than 1.5 fold-change upon suppression of ATRX, of which 233 genes were up-regulated and 512 genes were down-regulated (Figure 7B).

To explore the genes that are differentially expressed upon ATRX suppression, I used GSEA to identify enrichment of gene sets. Interestingly, one of the genes sets that was significantly enriched for upon ATRX suppression and immortalization is named ‘PID_Telomerase_pathway’ and contained several ALT-related protein such as TREF1/2 and members of the XRCC complex,

as well as nibrin (NBN) a member of the MRN complex which is essential for ALT activity (*6*). The up-regulation of ALT-associated genes upon ATRX suppression confirms the potential involvement of ATRX in ALT activation, and importantly suggests that more ALT-related genes can be identified by further mining the gene expression changes following ATRX suppression.

Searching for positive controls for suppression of ALT activity

Based on the literature, I tried to use genes that are known to be involved in ALT activity as positive controls for determining ALT inhibition in Aim 3. I obtained multiple shRNAs for each of the genes, however, in my hands and as shown in Figure 1B, I could not achieve a dynamic range that is sufficient for an HTS screen. Therefore, I am attempting to identify better positive controls for ALT activity suppression. Part of this search uses the gene expression data that I generated above to guide the selection of new potential positive controls. I am testing genes whose expression in ALT+ cells is significantly higher than in non-ALT cells. Identifying robust positive controls with a wide dynamic range is essential for the success of the screen, since it will determine the threshold of calling genes as hits in the screen, and therefore will determine the specificity (false positive rate) and sensitivity (false negative rate) of the screen.

Importantly, characterization of the proteins associated with PML and Sp100 (Aim 1) relays on the same positive control genes. According to the C-circle assay, the suppression of these genes resulted in only partial suppression of ALT activity. In order to reliably identify proteins associated with PML and Sp100 in ALT+ cells by mass-spectrometry analysis, it is essential to achieve a strong suppression of ALT activity in the perturbed samples. As described above, I am using the gene expression data to search for genes whose perturbation can lead to stronger suppression of ALT activity.

Key research accomplishments

- Calibrated a fluorescence-based C-circle assay to enable quantification and safe detection of ALT activity with moderate throughput.
- Tested the contribution of ATRX and DAXX suppression to ALT activation.
- Profiled gene expression patterns of 16 ALT+ cell-lines as well as 9 non-ALT cell-lines.
- Defined an ALT-related gene expression signature.
- Identified several sets of genes that are uniquely expressed in ALT+ cells and are potentially related to ALT activity.
- Identified small molecule inhibitors negatively connected to the ALT+ gene expression profile, with potential efficiency in ALT+ tumors.
- Profiled changes in gene expression upon suppression of ATRX.

Conclusion

In order to shed more light on the mechanism that lead to ALT activation, I focused on changes in gene expression upon ALT activation by profiling the transcriptome of 16 ALT+ cell-lines and 9 non-ALT cell-lines. By applying unbiased analysis strategy, I showed that ALT activity imposes a significant and wide effect on global gene expression patterns. Further analysis revealed an ALT+ differential gene expression signature that contained multiple genes that are already known to be involved in ALT activity. Mining the ALT-related expression signature using Gene Set Enrichment Analysis identified several sets of genes with potential relevance to ALT activity. Interestingly, many of these genes regulate DNA replication, the cell-cycle, and DNA damage repair. The up-regulation of those genes in ALT+ cell-lines suggests that ALT activity involves re-wiring of these exiting mechanisms to elongate and maintain telomeres in the absence of telomerase. It could also indicate potential dependencies of ALT+ cells, such as increased DNA damage repair activity, in line with our previous observation of high level of genomic instability and frequent presence of DNA damage in ALT+ cells (*16*). Querying the connectivity map dataset with the ALT+ signature identified few small molecule inhibitors that could have increased efficiency in ALT+ breast cancer tumors.

ATRX is a chromatin modulator that was shown to be genetically and functionally altered in ALT+ tumors. Never the less, its suppression was not sufficient to induce immortalization of BJ cells, suggesting that additional factors are required. To study the cellular events that occur upon loss of ATRX function, I profiled global gene expression from BJ cells that were immortalized upon knock-down of ATRX. GSEA analysis identified a set of genes that contains several ALT-related genes, thus enabling a focused search within this gene set for ATRX-depended ALT-regulating genes.

The high level of genomic instability and frequent presence of DNA damage foci observed by us in ALT cells (*16*), suggests that these cells will have unique vulnerabilities, which are yet to be found.

Together, or comprehensive study of the genomic features of ALT cells (*16*) and the broad profiling of the ALT-related gene expression are useful resources for further studying the mechanism that regulates and facilitates ALT activity. Several of the gene sets identified here include known drug targets and thus could have important clinical implications.

Publications, Abstracts and Presentations

Lovejoy CA, Li W, Reisenweber S, Thongthip S, Bruno J, de Lange T, De S, Petrini JH, Sung PA, Jasin M, Rosenbluh J, **Zwang Y**, Weir BA, Hatton C, Ivanova E, Macconaill L, Hanna M, Hahn WC, Lue NF, Reddel RR, Jiao Y, Kinzler K, Vogelstein B, Papadopoulos N, Meeker AK, Consortium ALTSC (2012) Loss of ATRX, genome instability, and an altered DNA damage response are hallmarks of the alternative lengthening of telomeres pathway. PLoS genetics 8: e1002772

Inventions, Patents and Licenses

Nothing to report

Reportable outcomes

Nothing to report

Other achievements

Nothing to report

Opportunities for training and professional development

Training:

Weekly scientific updating meetings with mentor and group members to discuss my progress as well as other projects conducted in the group. Since several group members are physician-scientists many of the discussions were focused on the relevance of the project and results to cancer detection and therapy.

Bi-weekly ono-on-one meetings with mentor to review results, design experimental strategy, and discuss progress.

Professional development:

One day workshops on bioinformatics tools given by developer teams at the Broad Institute: GSEA, Gene-E, IGV, Firehose, GenePattern.

A week-long workshop on gene-expression analysis and relevant statistical tools given by computational-biology scientists at the Broad Institute.

Cancer Dependencies working group seminars: monthly seminars on current research and data analysis on cancer dependencies, potential targets, and therapies.

References

1. A. Queisser, S. Heeg, M. Thaler, A. von Werder, O. G. Opitz, Inhibition of telomerase induces alternative lengthening of telomeres during human esophageal carcinogenesis. *Cancer genetics* **206**, 374-386 (2013); published online EpubNov (10.1016/j.cancergen.2013.10.001).
2. R. Villa, M. Folini, P. Perego, R. Supino, E. Setti, M. G. Daidone, F. Zunino, N. Zaffaroni, Telomerase activity and telomere length in human ovarian cancer and melanoma cell lines: correlation with sensitivity to DNA damaging agents. *International journal of oncology* **16**, 995-1002 (2000); published online EpubMay (
3. A. J. Cesare, R. R. Reddel, Alternative lengthening of telomeres: models, mechanisms and implications. *Nature reviews. Genetics* **11**, 319-330 (2010); published online EpubMay (10.1038/nrg2763).
4. A. P. Subhawong, C. M. Heaphy, P. Argani, Y. Konishi, N. Kouprina, H. Nassar, R. Vang, A. K. Meeker, The alternative lengthening of telomeres phenotype in breast carcinoma is associated with HER-2 overexpression. *Modern pathology : an official journal of the United States and Canadian Academy of Pathology, Inc* **22**, 1423-1431 (2009); published online EpubNov (10.1038/modpathol.2009.125).
5. B. Xu, M. Peng, Q. Song, The co-expression of telomerase and ALT pathway in human breast cancer tissues. *Tumour biology : the journal of the International Society for Oncodevelopmental Biology and Medicine* **35**, 4087-4093 (2014); published online EpubMay (10.1007/s13277-013-1534-0).
6. W. Q. Jiang, Z. H. Zhong, J. D. Henson, A. A. Neumann, A. C. Chang, R. R. Reddel, Suppression of alternative lengthening of telomeres by Sp100-mediated sequestration of the MRE11/RAD50/NBS1 complex. *Molecular and cellular biology* **25**, 2708-2721 (2005); published online EpubApr (10.1128/MCB.25.7.2708-2721.2005).
7. P. R. Potts, H. Yu, The SMC5/6 complex maintains telomere length in ALT cancer cells through SUMOylation of telomere-binding proteins. *Nature structural & molecular biology* **14**, 581-590 (2007); published online EpubJul (10.1038/nsmb1259).
8. S. Zeng, T. Xiang, T. K. Pandita, I. Gonzalez-Suarez, S. Gonzalo, C. C. Harris, Q. Yang, Telomere recombination requires the MUS81 endonuclease. *Nature cell biology* **11**, 616-623 (2009); published online EpubMay (10.1038/ncb1867).
9. C. M. Heaphy, R. F. de Wilde, Y. Jiao, A. P. Klein, B. H. Edil, C. Shi, C. Bettegowda, F. J. Rodriguez, C. G. Eberhart, S. Hebbar, G. J. Offerhaus, R. McLendon, B. A. Rasheed, Y. He, H. Yan, D. D. Bigner, S. M. Oba-Shinjo, S. K. Marie, G. J. Riggins, K. W. Kinzler, B. Vogelstein, R. H. Hruban, A. Maitra, N. Papadopoulos, A. K. Meeker, Altered telomeres in tumors with ATRX and DAXX mutations. *Science* **333**, 425 (2011); published online EpubJul 22 (10.1126/science.1207313).
10. J. Schwartzentruber, A. Korshunov, X. Y. Liu, D. T. Jones, E. Pfaff, K. Jacob, D. Sturm, A. M. Fontebasso, D. A. Quang, M. Tonjes, V. Hovestadt, S. Albrecht, M. Kool, A. Nantel, C. Konermann, A. Lindroth, N. Jager, T. Rausch, M. Ryzhova, J. O. Korbel, T. Hielscher, P. Hauser, M. Garami, A. Klekner, L. Bognar, M. Ebinger, M. U. Schuhmann, W. Scheurlen, A. Pekrun, M. C. Fruhwald, W. Roggendorf, C. Kramm, M. Durken, J. Atkinson, P. Lepage, A. Montpetit, M. Zakrzewska, K. Zakrzewski, P. P. Liberski, Z. Dong, P. Siegel, A. E. Kulozik, M. Zapatka, A. Guha, D. Malkin, J. Felsberg, G. Reifenberger, A. von Deimling, K. Ichimura, V. P. Collins, H. Witt, T. Milde, O. Witt, C. Zhang, P. Castelo-Branco, P. Lichter, D. Faury, U. Tabori, C. Plass, J. Majewski, S. M. Pfister, N. Jabado, Driver mutations in histone H3.3 and chromatin remodelling genes in paediatric glioblastoma. *Nature* **482**, 226-231 (2012); published online EpubFeb 9 (10.1038/nature10833).
11. J. C. Lee, Y. M. Jeng, J. Y. Liau, J. H. Tsai, H. H. Hsu, C. Y. Yang, Alternative lengthening of telomeres and loss of ATRX are frequent events in pleomorphic and dedifferentiated liposarcomas.

Modern pathology : an official journal of the United States and Canadian Academy of Pathology, Inc, (2015); published online EpubMay 29 (10.1038/modpathol.2015.67).

12. C. E. Napier, L. I. Huschtscha, A. Harvey, K. Bower, J. R. Noble, E. A. Hendrickson, R. R. Reddel, ATRX represses alternative lengthening of telomeres. *Oncotarget*, (2015); published online EpubApr 15 (
13. P. Drane, K. Ouararhni, A. Depaux, M. Shuaib, A. Hamiche, The death-associated protein DAXX is a novel histone chaperone involved in the replication-independent deposition of H3.3. *Genes & development* **24**, 1253-1265 (2010); published online EpubJun 15 (10.1101/gad.566910).
14. P. W. Lewis, S. J. Elsaesser, K. M. Noh, S. C. Stadler, C. D. Allis, Daxx is an H3.3-specific histone chaperone and cooperates with ATRX in replication-independent chromatin assembly at telomeres. *Proceedings of the National Academy of Sciences of the United States of America* **107**, 14075-14080 (2010); published online EpubAug 10 (10.1073/pnas.1008850107).
15. L. H. Wong, J. D. McGhie, M. Sim, M. A. Anderson, S. Ahn, R. D. Hannan, A. J. George, K. A. Morgan, J. R. Mann, K. H. Choo, ATRX interacts with H3.3 in maintaining telomere structural integrity in pluripotent embryonic stem cells. *Genome research* **20**, 351-360 (2010); published online EpubMar (10.1101/gr.101477.109).
16. C. A. Lovejoy, W. Li, S. Reisenweber, S. Thongthip, J. Bruno, T. de Lange, S. De, J. H. Petrini, P. A. Sung, M. Jasin, J. Rosenbluh, Y. Zwang, B. A. Weir, C. Hatton, E. Ivanova, L. Macconaill, M. Hanna, W. C. Hahn, N. F. Lue, R. R. Reddel, Y. Jiao, K. Kinzler, B. Vogelstein, N. Papadopoulos, A. K. Meeker, A. L. T. S. C. Consortium, Loss of ATRX, genome instability, and an altered DNA damage response are hallmarks of the alternative lengthening of telomeres pathway. *PLoS genetics* **8**, e1002772 (2012)10.1371/journal.pgen.1002772).
17. B. Luke, J. Lingner, TERRA: telomeric repeat-containing RNA. *The EMBO journal* **28**, 2503-2510 (2009); published online EpubSep 2 (10.1038/emboj.2009.166).
18. L. J. Ng, J. E. Cropley, H. A. Pickett, R. R. Reddel, C. M. Suter, Telomerase activity is associated with an increase in DNA methylation at the proximal subtelomere and a reduction in telomeric transcription. *Nucleic acids research* **37**, 1152-1159 (2009); published online EpubMar (10.1093/nar/gkn1030).
19. D. Clynes, C. Jelinska, B. Xella, H. Ayyub, S. Taylor, M. Mitson, C. Z. Bachrati, D. R. Higgs, R. J. Gibbons, ATRX dysfunction induces replication defects in primary mouse cells. *PloS one* **9**, e92915 (2014)10.1371/journal.pone.0092915).
20. M. Reich, T. Liefeld, J. Gould, J. Lerner, P. Tamayo, J. P. Mesirov, GenePattern 2.0. *Nature genetics* **38**, 500-501 (2006); published online EpubMay (10.1038/ng0506-500).
21. J. Gould, G. Getz, S. Monti, M. Reich, J. P. Mesirov, Comparative gene marker selection suite. *Bioinformatics* **22**, 1924-1925 (2006); published online EpubAug 1 (10.1093/bioinformatics/btl196).
22. A. Saharia, S. A. Stewart, FEN1 contributes to telomere stability in ALT-positive tumor cells. *Oncogene* **28**, 1162-1167 (2009); published online EpubFeb 26 (10.1038/onc.2008.458).
23. L. Sun, D. Li, X. Dong, H. Yu, J. T. Dong, C. Zhang, X. Lu, J. Zhou, Small-molecule inhibition of Aurora kinases triggers spindle checkpoint-independent apoptosis in cancer cells. *Biochemical pharmacology* **75**, 1027-1034 (2008); published online EpubMar 1 (10.1016/j.bcp.2007.11.007).
24. A. Romanelli, A. Clark, F. Assayag, S. Chateau-Joubert, M. F. Poupon, J. L. Servely, J. J. Fontaine, X. Liu, E. Spooner, S. Goodstal, P. de Cremoux, I. Bieche, D. Decaudin, E. Marangoni, Inhibiting aurora kinases reduces tumor growth and suppresses tumor recurrence after chemotherapy in patient-derived triple-negative breast cancer xenografts. *Molecular cancer therapeutics* **11**, 2693-2703 (2012); published online EpubDec (10.1158/1535-7163.MCT-12-0441-T).
25. P. Finetti, N. Cervera, E. Charafe-Jauffret, C. Chabannon, C. Charpin, M. Chaffanet, J. Jacquemier, P. Viens, D. Birnbaum, F. Bertucci, Sixteen-kinase gene expression identifies luminal breast cancers with poor prognosis. *Cancer research* **68**, 767-776 (2008); published online EpubFeb 1 (10.1158/0008-5472.CAN-07-5516).

26. Z. Q. Wu, X. Yang, G. Weber, X. Liu, Plk1 phosphorylation of TRF1 is essential for its binding to telomeres. *The Journal of biological chemistry* **283**, 25503-25513 (2008); published online EpubSep 12 (10.1074/jbc.M803304200).
27. X. Dai, C. Huang, W. Chai, CDK1 differentially regulates G-overhang generation at leading- and lagging-strand telomeres in telomerase-negative cells in G2 phase. *Cell cycle* **11**, 3079-3086 (2012); published online EpubAug 15 (10.4161/cc.21472).
28. M. McKerlie, J. R. Walker, T. R. Mitchell, F. R. Wilson, X. D. Zhu, Phosphorylated (pT371)TRF1 is recruited to sites of DNA damage to facilitate homologous recombination and checkpoint activation. *Nucleic acids research* **41**, 10268-10282 (2013); published online EpubDec (10.1093/nar/gkt775).
29. J. Lamb, E. D. Crawford, D. Peck, J. W. Modell, I. C. Blat, M. J. Wrobel, J. Lerner, J. P. Brunet, A. Subramanian, K. N. Ross, M. Reich, H. Hieronymus, G. Wei, S. A. Armstrong, S. J. Haggarty, P. A. Clemons, R. Wei, S. A. Carr, E. S. Lander, T. R. Golub, The Connectivity Map: using gene-expression signatures to connect small molecules, genes, and disease. *Science* **313**, 1929-1935 (2006); published online EpubSep 29 (10.1126/science.1132939).
30. F. H. Chung, Y. R. Chiang, A. L. Tseng, Y. C. Sung, J. Lu, M. C. Huang, N. Ma, H. C. Lee, Functional Module Connectivity Map (FMCM): a framework for searching repurposed drug compounds for systems treatment of cancer and an application to colorectal adenocarcinoma. *PloS one* **9**, e86299 (2014)10.1371/journal.pone.0086299).
31. D. A. Yardley, R. R. Ismail-Khan, B. Melichar, M. Lichinitser, P. N. Munster, P. M. Klein, S. Cruickshank, K. D. Miller, M. J. Lee, J. B. Trepel, Randomized phase II, double-blind, placebo-controlled study of exemestane with or without entinostat in postmenopausal women with locally recurrent or metastatic estrogen receptor-positive breast cancer progressing on treatment with a nonsteroidal aromatase inhibitor. *Journal of clinical oncology : official journal of the American Society of Clinical Oncology* **31**, 2128-2135 (2013); published online EpubJun 10 (10.1200/JCO.2012.43.7251).

Appendix

A copy of paper that included parts of the work reported here:

Lovejoy CA, Li W, Reisenweber S, Thongthip S, Bruno J, de Lange T, De S, Petrini JH, Sung PA, Jasin M, Rosenbluh J, **Zwang Y**, Weir BA, Hatton C, Ivanova E, Macconaill L, Hanna M, Hahn WC, Lue NF, Reddel RR, Jiao Y, Kinzler K, Vogelstein B, Papadopoulos N, Meeker AK, Consortium ALTSC (2012) Loss of ATRX, genome instability, and an altered DNA damage response are hallmarks of the alternative lengthening of telomeres pathway. PLoS genetics 8: e1002772

Supporting data

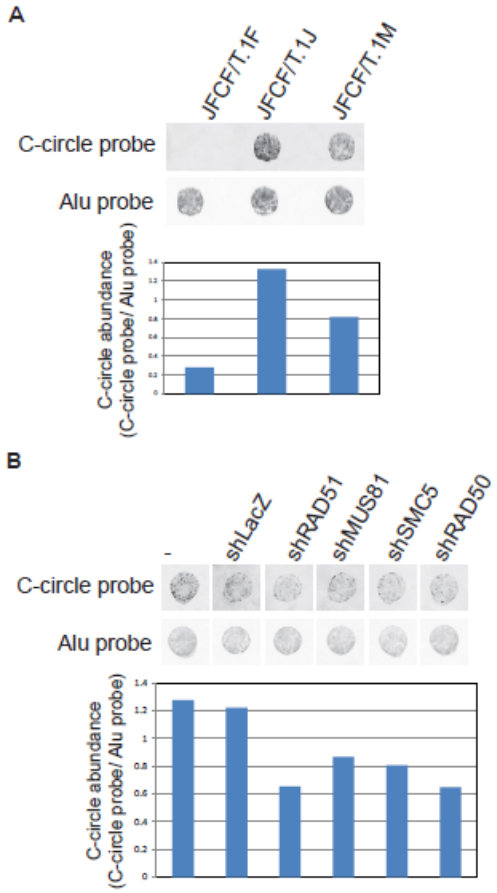

Figure 1

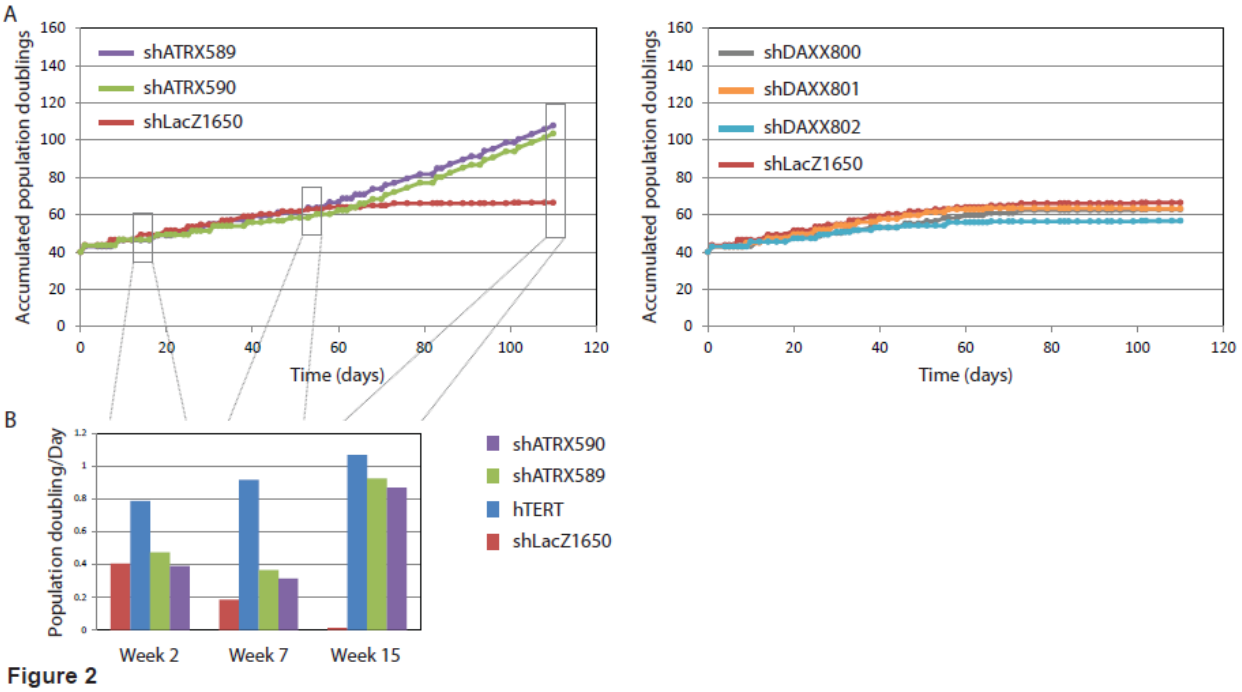
A
Accumulated population doublings
shATRX589
shATRX590
shLacZ1650
Time (days)
shDAXX800
shDAXX801
shDAXX802
shLacZ1650
Time (days)

B
Population doubling/Day
Week 2
Week 7
Week 15
shATRX590
shATRX589
hTERT
shLacZ1650

Figure 2

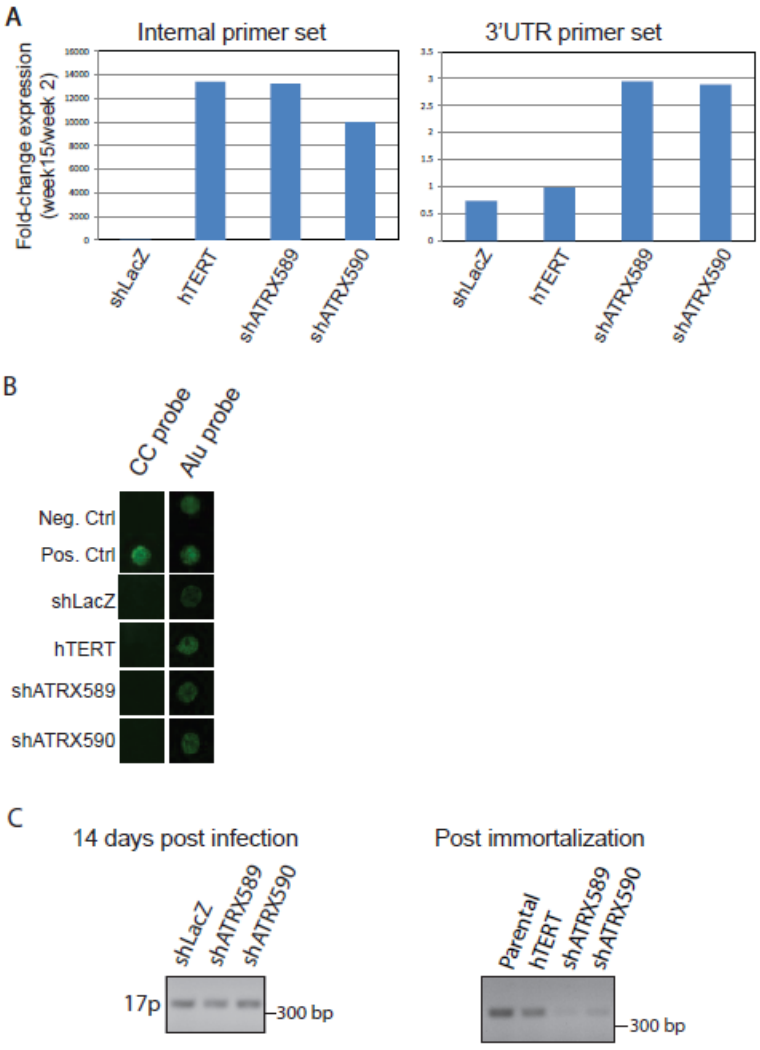
A
Internal primer set
3'UTR primer set
Fold-change expression (week15/week 2)
shLacZ
hTERT
shATRX589
shATRX590
B
CC probe
Alu probe
Neg. Ctrl
Pos. Ctrl
shLacZ
hTERT
shATRX589
shATRX590
C
14 days post infection
shLacZ
shATRX589
shATRX590
17p
300 bp
Post immortalization
Parental
hTERT
shATRX589
shATRX590
300 bp

Figure 3

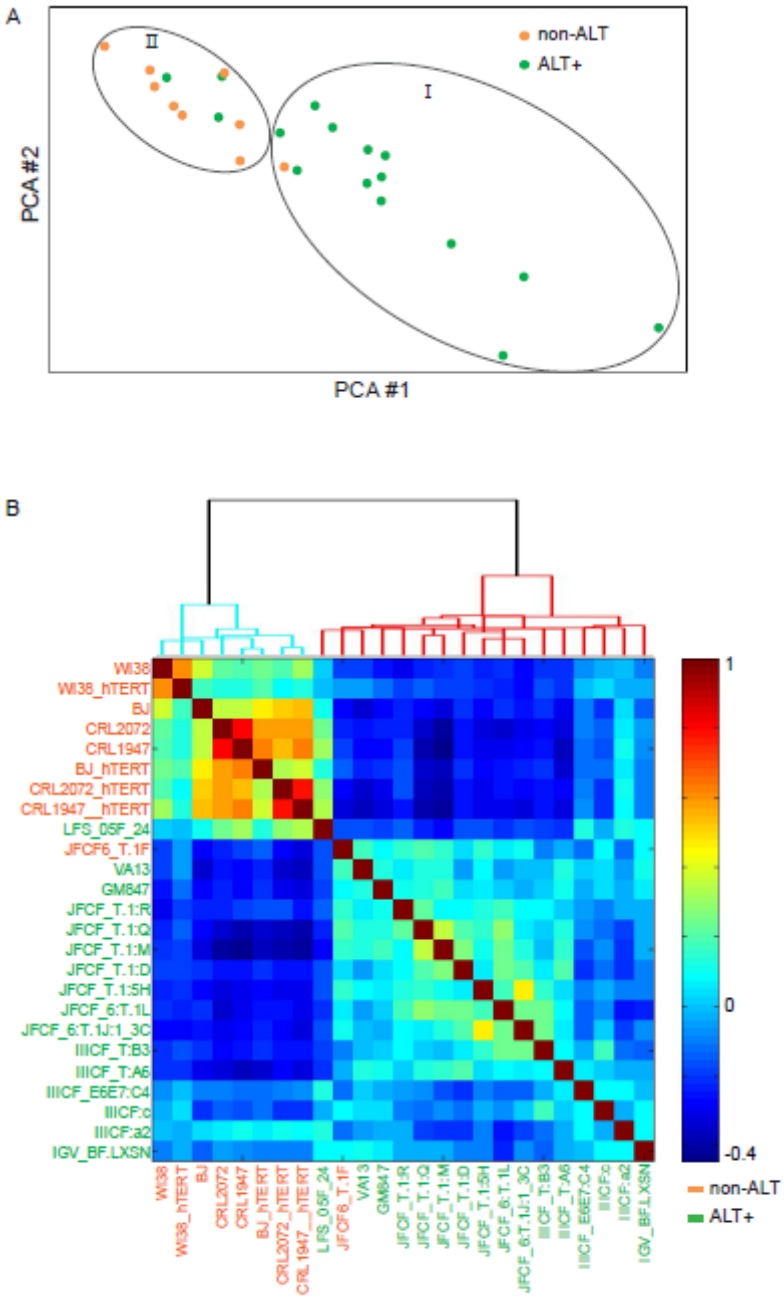
A
non-ALT
ALT+
II
I
PCA #2
PCA #1
B
WI38
WI38_hTERT
BJ
CRL2072
CRL1947
BJ_hTERT
CRL2072_hTERT
CRL1947__hTERT
LFS_05F_24
JFCF6_T.1F
VA13
GM847
JFCF_T.1:R
JFCF_T.1:Q
JFCF_T.1:M
JFCF_T.1:D
JFCF_T.1:5H
JFCF_6:T.1L
JFCF_6:T.1J:1_3C
IIICF_T:B3
IIICF_T:A6
IIICF_E6E7:C4
IIICF:c
IIICF:a2
IGV_BF.LXSN
1
0
-0.4
non-ALT
ALT+

Figure 4

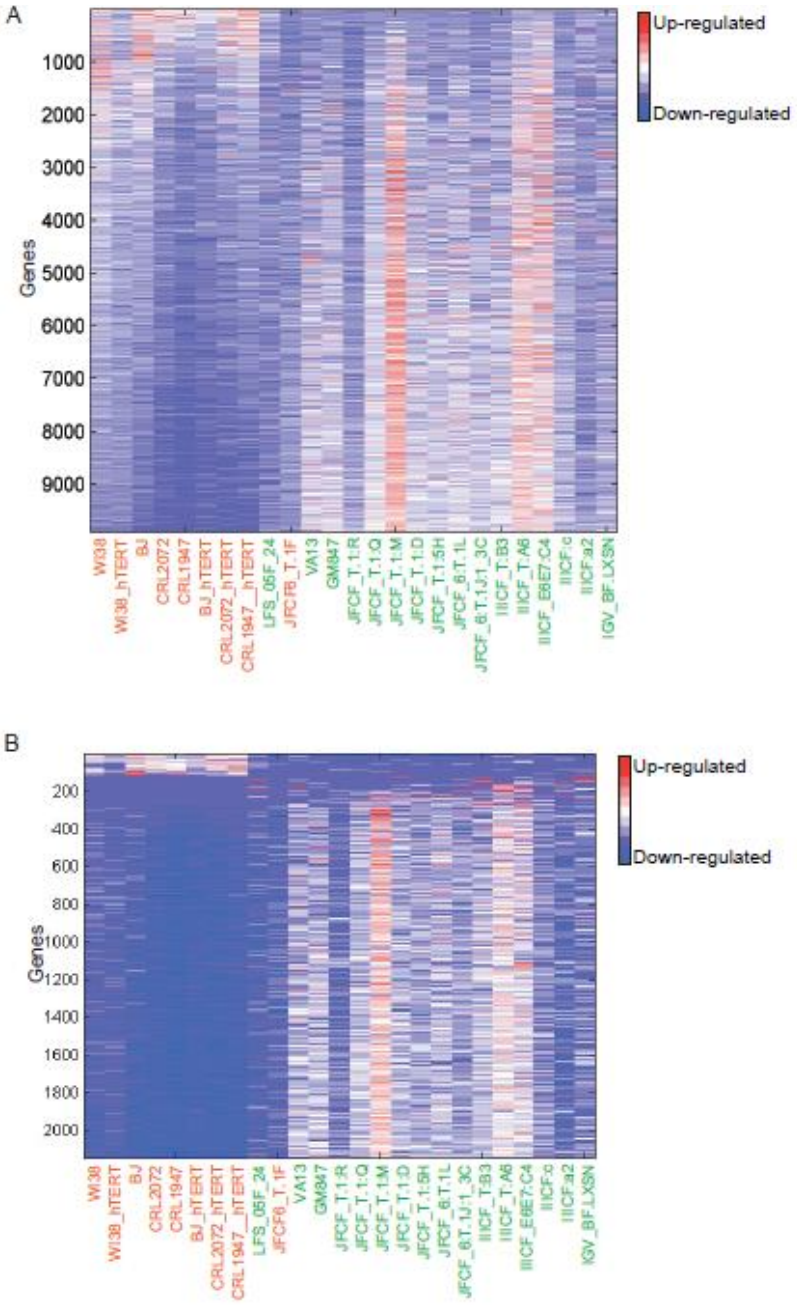
A
Up-regulated
Down-regulated
Genes
1000
2000
3000
4000
5000
6000
7000
8000
9000
WI38
WI38_hTERT
BJ
CRL2072
CRL1947
BJ_hTERT
CRL2072_hTERT
CRL1947__hTERT
LFS_05F_24
JFCF8_T_1F
VA13
GM847
JFCF_T.1:R
JFCF_T.1:Q
JFCF_T.1:M
JFCF_T.1:D
JFCF_T.1:5H
JFCF_6.T.1L
JFCF_6.T.1J:1_3C
IIICF_T:B3
IIICF_T:A6
IIICF_E6E7:C4
IIICF:c
IIICF:a2
IGV_BF.LXSN
B
Up-regulated
Down-regulated
Genes
200
400
600
800
1000
1200
1400
1600
1800
2000
WI38
WI38_hTERT
BJ
CRL2072
CRL1947
BJ_hTERT
CRL2072_hTERT
CRL1947__hTERT
LFS_05F_24
JFCF8_T_1F
VA13
GM847
JFCF_T.1:R
JFCF_T.1:Q
JFCF_T.1:M
JFCF_T.1:D
JFCF_T.1:5H
JFCF_6.T.1L
JFCF_6.T.1J:1_3C
IIICF_T:B3
IIICF_T:A6
IIICF_E6E7:C4
IIICF:c
IIICF:a2
IGV_BF.LXSN

Figure 5

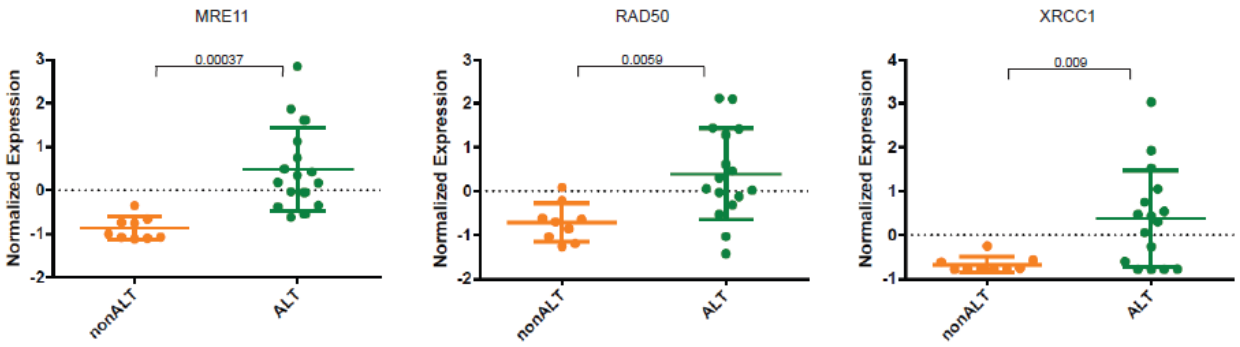

Figure 5 cont.

A. GO: ATP DEPENDENT DNA HELICASE ACTIVITY

B. REACTOME: PROCESSIVE SYNTHESIS ON THE LAGGING STRAND

C. KEGG: MISMATCH REPAIR

D. FINETTI BREAST CANCER KINOME RED

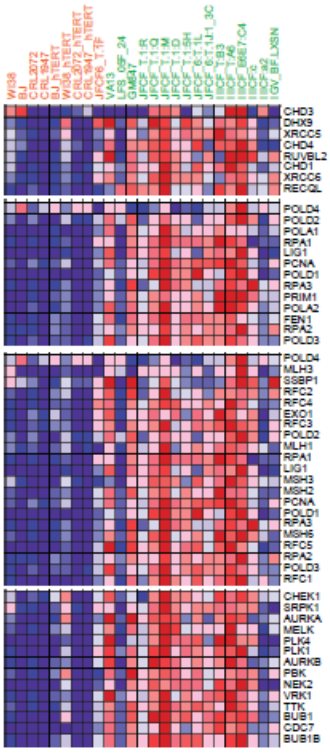

Figure 6

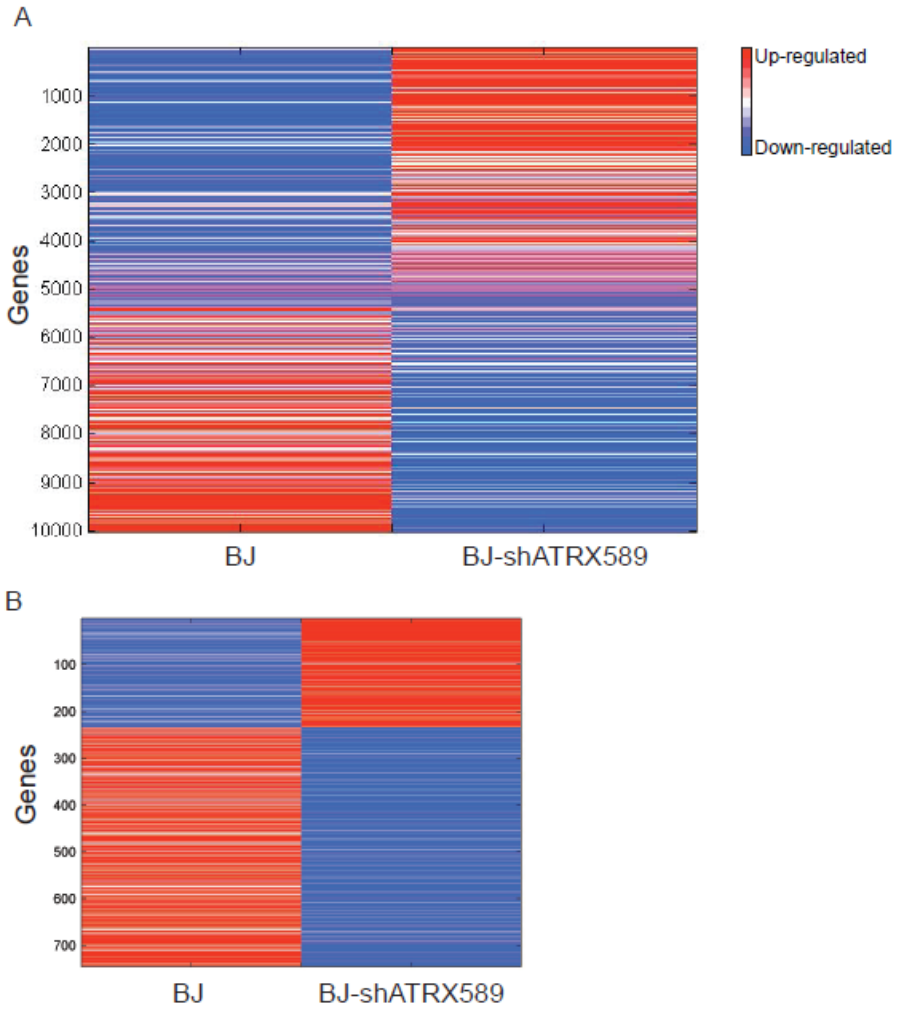
A
Up-regulated
Down-regulated
Genes
1000
2000
3000
4000
5000
6000
7000
8000
9000
10000
BJ
BJ-shATRX589
B
Genes
100
200
300
400
500
600
700
BJ
BJ-shATRX589

Figure 7

NAME	SIZE	NES
MITOTIC SISTER CHROMATID SEGREGATION	11	-0.77373
SISTER CHROMATID SEGREGATION	11	-0.77373
ATP DEPENDENT DNA HELICASE ACTIVITY	8	-0.74028
G1 PHASE OF MITOTIC CELL CYCLE	8	-0.71781
REPLICATION FORK	14	-0.7006
ORGANELLAR SMALL RIBOSOMAL SUBUNIT	8	-0.68236
MITOCHONDRIAL SMALL RIBOSOMAL SUBUNIT	8	-0.68236
SMALL RIBOSOMAL SUBUNIT	8	-0.68236
CHROMOSOME SEGREGATION	20	-0.67529
REGULATION OF MITOSIS	28	-0.6676
SPINDLE MICROTUBULE	15	-0.66266
MICROTUBULE MOTOR ACTIVITY	12	-0.65116
KINETOCHORE	20	-0.64197
DNA DEPENDENT ATPASE ACTIVITY	17	-0.63868
MITOTIC CELL CYCLE CHECKPOINT	16	-0.63795
G1 PHASE	9	-0.63567
DNA DIRECTED DNA POLYMERASE ACTIVITY	12	-0.62905
MICROTUBULE ORGANIZING CENTER ORGANIZATION AND BIOGENESIS	9	-0.62795
DRUG BINDING	10	-0.62713
DNA POLYMERASE ACTIVITY	14	-0.62648

Table 1: Top 20 GO gene sets enriched for in ALT+ cell-lines. Size indicates the number of genes included in each set. NES, Normalized Enrichment Score. Reflecting the degree to which a gene set is over-represented at either ends of the ranked list, normalized by permutations of the ranked dataset. A more negative NES indicates higher enrichment of the gene set in the ALT+ differentially up-regulated end of the ranked list.

NAME	SIZE	NES
REACTOME PROCESSIVE SYNTHESIS ON THE LAGGING STRAND	13	-0.89422
REACTOME REMOVAL OF THE FLAP INTERMEDIATE FROM THE C STRAND	9	-0.89365
REACTOME LAGGING STRAND SYNTHESIS	17	-0.79381
REACTOME POL SWITCHING	12	-0.79306
LY AGING MIDDLE DN	16	-0.79292
KANG DOXORUBICIN RESISTANCE UP	47	-0.78178
AMUNDSON GAMMA RADIATION RESPONSE	34	-0.77391
FINETTI BREAST CANCER KINOME RED	14	-0.76779
KALMA E2F1 TARGETS	11	-0.75699
MONTERO THYROID CANCER POOR SURVIVAL UP	10	-0.75409
REACTOME PURINE RIBONUCLEOSIDE MONOPHOSPHATE BIOSYNTHESIS	9	-0.75289
KUMAMOTO RESPONSE TO NUTLIN 3A DN	9	-0.7507
BURTON ADIPOGENESIS PEAK AT 24HR	25	-0.74505
REACTOME REPAIR SYNTHESIS FOR GAP FILLING BY DNA POL IN TC NER	14	-0.74457
KEGG MISMATCH REPAIR	21	-0.744
TANG SENESCENCE TP53 TARGETS DN	45	-0.7432
KAMMINGA EZH2 TARGETS	34	-0.73923
CROONQUIST NRAS SIGNALING DN	66	-0.73693
REACTOME SLBP DEPENDENT PROCESSING OF REPLICATION DEPENDENT HISTONE PRE MRNAS	8	-0.73269
CROONQUIST IL6 DEPRIVATION DN	80	-0.7323

Table 2: Top 20 curated gene sets enriched for in ALT+ cell-lines.

Name	Enrichment score	p-value
tyrphostin AG-825	-0.967	---
piperlongumine	-0.961	0.0033
dexverapamil	-0.959	---
MS-275	-0.946	0.00634
celastrol	-0.946	---
menadione	-0.913	0.01521
trazodone	-0.891	0.00248
fisetin	-0.888	---
ebselen	-0.868	0.00457
1,4-chrysenequinone	-0.868	0.03455
GW-8510	-0.867	0.00062
cantharidin	-0.864	---
rottlerin	-0.861	0.00547
blebbistatin	-0.854	0.04269
luteolin	-0.853	0.00084
clomipramine	-0.85	0.00093
thioguanosine	-0.85	0.00093
apigenin	-0.849	0.00095
sulconazole	-0.845	0.00103
triflusal	-0.839	0.00841

Table 3: Top 20 small compound perturbations negatively connected to the ALT+ gene expression signature. Enrichment score represents the strength of connectivity.

Legend to figures

Figure 1: Calibration a fluorescence-based C-circle assay. **A**. Genomic DNA was isolated from the indicated cells. Following C-circle assay reaction, samples were dot-blotted, and an IRDye-labeled probe specific for either C-circle assay product or Alu repeats was hybridized to the membranes. Membranes were scanned using LiCor Odessey imaging system, and dotes quantified using Image Studio software. Bar-graph presents relative abundance of C-circles. **B**. indicated shRNAs were virally delivered into U2OS cells, followed by 2 days of puromycin selection and additional 2 days propagation under normal culture conditions. Genomic DNA was then isolated, and C-circle assay performed and quantified as in A.

Figure 2: Immortalization of BJ cells upon knock-down of ATRX and DAXX. **A**. BJ cells were infected with LacZ- ATRX- or DAXX-specific shRNAs at population-doubling (PD) 40. Cells were selected for 2 days with puromycin, and at least $1\text{^}7$ cells for each sub-line were maintained in culture for 110 days. Cultures were split at <80% confluence, and growth media was re-freshed every 3 days. Cells were counted at each culture passaging and accumulated PD was recorded. **B**. Rate of population-doubling per day is plotted for the indicated sub-lines at the indicated times, corresponding to boxed time-points in A.

Figure 3: Characterizing telomere maintenance mechanism of the two immortalized shATRX colonies. **A**. RNA was isolated from the indicated sub-lines at weeks 2 and 15 (see Figure 2A). hTERT expression was measured using qPCR with either an internal primer set designed around exons 5 and 6, or a 3'UTR primer set designed around the last exon and the 3'UTR of the endogenous gene. Shown is fold-change of expression level at week 15 compared to week 2 for the two probe sets. **B**. genomic DNA was isolated at week 15 from the indicated sub-lines (see Figure 2A). Shown are dot-blots of the C-circle probe and Alu probe. JFCF/T.1F and JFCF/T.1J were used as negative and positive controls, respectively. **C**. RNA was isolated from the indicated sub-lines 14 days after infection or after immortalized colonies emerged in the shATRX sub-lines. TERRA-specific cDNA was synthesized and TERRA expressed from chromosome 17p was amplified.

Figure 4: Analysis of gene expression profiles of ALT+ and non-ALT cell-lines shows significant ALT-related difference in global gene expression. **A.** PCA analysis of normalized expression data. The values for the PCAs with the highest variance are plotted for each cell-line. Green, ALT+ cell-lines; Orange, non-ALT cell-lines. The circles labeled I and II mark the two identified clusters. **B.** Correlation coefficients were calculated for all variable genes across all cell-lines and plotted as a heatmap. Red, positive correlation; Blue, Negative correlation. Dendrogram above corresponds to the degree of linkage between cell-lines.

Figure 5: Comparative Marker Selection analysis defines an ALT-related gene signature. **A.** Plotted is the expression of genes across all cell-lines ranked according to the correlation between the gene's expression and the phenotypic classification of the cell-lines. Red, up-regulated; Blue,

down-regulated. **B.** The expression of the 2147 most significantly differentially expressed genes according to the Comparative Marker Selection analysis is plotted. **C-E.** Expression of known ALT-related genes is compared between non-ALT and ALT+ cell-lines. Mean and SD indicated by bar, p-value for differential expression (T-test) is presented.

Figure 6: GSEA reveals potential associations to ALT activity. **A-D**. Expression of genes included in the indicated enriched gene sets across all cell-lines. Heatmap colors as in Figure 5A.

Figure 7: Gene expression profiling of cells immortalized by ATRX knock-down. **A**. Gene expression of parental BJ cells and BJ-shATRX589 immortalized cells. Genes ranked-ordered according to their expression fold-change following suppression of ATRX. Red, up-regulated; Blue, down-regulated. **B.** Expression of genes exhibiting over 1.5 fold-change upon ATRX knock-down.

OPEN ACCESS Freely available online

PLoS GENETICS

Loss of ATRX, Genome Instability, and an Altered DNA Damage Response Are Hallmarks of the Alternative Lengthening of Telomeres Pathway

Courtney A. Lovejoy[1], Wendi Li[1], Steven Reisenweber[1], Supawat Thongthip[1], Joanne Bruno[1], Titia de Lange[1]*, Saurav De[2], John H. J. Petrini[2], Patricia A. Sung[3], Maria Jasin[3], Joseph Rosenbluh[4], Yaara Zwang[4,5], Barbara A. Weir[4], Charlie Hatton[5], Elena Ivanova[5], Laura Macconaill[5], Megan Hanna[5], William C. Hahn[4,5], Neal F. Lue[6], Roger R. Reddel[7,8], Yuchen Jiao[9], Kenneth Kinzler[9], Bert Vogelstein[9,10], Nickolas Papadopoulos[9], Alan K. Meeker[11], for the ALT Starr Cancer Consortium

1 Laboratory for Cell Biology and Genetics, The Rockefeller University, New York, New York, United States of America, **2** Molecular Biology Program, Sloan-Kettering Institute, Memorial Sloan-Kettering Cancer Center, New York, New York, United States of America, **3** Developmental Biology Program, Sloan-Kettering Institute, Memorial Sloan-Kettering Cancer Center, New York, New York, United States of America, **4** Broad Institute of Harvard and MIT, Cambridge, Massachusetts, United States of America, **5** Department of Medical Oncology, Dana-Farber Cancer Institute, Boston, Massachusetts, United States of America, **6** Department of Microbiology and Immunology, W. R. Hearst Microbiology Research Center, Weill Medical College, Cornell University, New York, New York, United States of America, **7** Children's Medical Research Institute, Westmead, New South Wales, Australia, **8** Sydney Medical School, University of Sydney, Sydney, New South Wales, Australia, **9** Ludwig Center for Cancer Genetics and Therapeutics, Johns Hopkins Sidney Kimmel Cancer Center, Baltimore, Maryland, United States of America, **10** Howard Hughes Medical Institutions, Johns Hopkins Sidney Kimmel Cancer Center, Baltimore, Maryland, United States of America, **11** Department of Pathology, Johns Hopkins University School of Medicine, Baltimore, Maryland, United States of America

Abstract

The Alternative Lengthening of Telomeres (ALT) pathway is a telomerase-independent pathway for telomere maintenance that is active in a significant subset of human cancers and in vitro immortalized cell lines. ALT is thought to involve templated extension of telomeres through homologous recombination, but the genetic or epigenetic changes that unleash ALT are not known. Recently, mutations in the ATRX/DAXX chromatin remodeling complex and histone H3.3 were found to correlate with features of ALT in pancreatic neuroendocrine cancers, pediatric glioblastomas, and other tumors of the central nervous system, suggesting that these mutations might contribute to the activation of the ALT pathway in these cancers. We have taken a comprehensive approach to deciphering ALT by applying genomic, molecular biological, and cell biological approaches to a panel of 22 ALT cell lines, including cell lines derived in vitro. Here we show that loss of ATRX protein and mutations in the *ATRX* gene are hallmarks of ALT–immortalized cell lines. In addition, ALT is associated with extensive genome rearrangements, marked micronucleation, defects in the G2/M checkpoint, and altered double-strand break (DSB) repair. These attributes will facilitate the diagnosis and treatment of ALT positive human cancers.

Citation: Lovejoy CA, Li W, Reisenweber S, Thongthip S, Bruno J, et al. (2012) Loss of ATRX, Genome Instability, and an Altered DNA Damage Response Are Hallmarks of the Alternative Lengthening of Telomeres Pathway. PLoS Genet 8(7): e1002772. doi:10.1371/journal.pgen.1002772

Editor: Hamish S. Scott, SA Pathology, Australia

Received February 17, 2012; **Accepted** May 4, 2012; **Published** July 19, 2012

Copyright: © 2012 Lovejoy et al. This is an open-access article distributed under the terms of the Creative Commons Attribution License, which permits unrestricted use, distribution, and reproduction in any medium, provided the original author and source are credited.

Funding: This work was made possible by a grant from the Starr Cancer Consortium and grants from the NIH to TdL (GM049046 and CA076027), WCH, NFL, MJ, and JHJP. TdL is an American Cancer Society Research Professor. NP, BV, KK, and YJ are supported by The Virginia and D. K. Ludwig Fund for Cancer Research. RRR is supported by a Cancer Council NSW Program Grant. CAL and YZ are supported by DOD Breast Cancer Research Program Postdoctoral Fellowships. JR was supported by a NIH/NIA fellowship (F32GM090437). The funders had no role in study design, data collection and analysis, decision to publish, or preparation of the manuscript.

Competing Interests: The authors have declared that no competing interests exist.

* E-mail: delange@mail.rockefeller.edu

Introduction

In the absence of telomerase activity, telomeres shorten with cell division, ultimately leading to senescence. Hence, the development of human cancer is associated with an active telomere maintenance system that provides an infinite source of telomeric DNA to potentiate immortality. Although telomerase reactivation is the most common mechanism of telomeric repeat addition in cancers, a significant subset of human tumors employs a telomerase-independent telomere maintenance pathway, referred to as ALT [1].

The emerging view is that ALT maintains telomeres through homology-directed recombination (HDR) [2]. Supporting this view, ALT cells show an elevated frequency of sequence exchanges between telomeres [2–4], contain extrachromosomal linear and circular telomeric DNA [5–8], and often exhibit heterogeneously-sized telomeres [1], features consistent with hyperactive HDR. The extrachromosomal telomeric DNA has been proposed to serve as a template for the extension of telomeres by a recombination mechanism akin to Break Induced Replication (BIR) [9,10]. In addition, ALT cells often carry altered PML bodies (ALT-associated PML bodies, or APBs) that contain telomeric DNA as well as numerous recombination factors [11]. Several proteins involved in recombination are known to be required for ALT, including the Mre11 complex, Mus81, and the SMC5/6 sumoylation pathway [6,12–15].

Author Summary

Telomeres, the protective elements at the ends of chromosomes, need to be maintained for cells to proliferate indefinitely. In many human cancers, the telomeric DNA is replenished by telomerase. However, a second pathway for telomere maintenance, referred to as the ALT pathway, has increasingly been recognized in human cancers. The genetic basis for activation of ALT is not known, but recent data have implicated a chromatin remodeling complex (ATRX/DAXX) and the histone variant H3.3 as players in the repression of ALT. We have examined a large panel of ALT cell lines for their genetic and cell biological features and found that loss of ATRX is a common event in the genesis of ALT lines. In addition, we document that ALT cell lines frequently undergo chromosomal changes and are impaired in their ability to detect and repair damage in their DNA. These hallmarks of ALT are expected to facilitate the detection of ALT–type tumors in the clinic and may lead to ALT–specific treatments.

ALT was discovered in a subset of immortalized cell lines that emerge at low frequency from human cell cultures in telomere crisis, but this pathway has increasingly been identified in human cancer. Approximately 10–15% of human cancers are suspected to use the ALT pathway based on their lack of telomerase activity in combination with certain hallmarks of ALT, such as the presence of extrachromosomal telomeric circles, APBs, and/or long and heterogeneous telomeres. Based on these criteria, ALT is relatively common in many sarcomas (osteosarcoma and some types of soft tissue sarcomas), certain endocrine tumors (pancreatic neuroendocrine tumors, paraganglioma), a subset of nervous system tumors (e.g. glioblastoma, medulloblastoma, oligodendroglioma, astrocytoma, ganglioneuroblastoma), bladder small cell carcinoma, and nonseminomatous germ cell tumors [16–18].

The molecular basis for the activation of the ALT pathway is not known. In vitro, the frequency of conversion to ALT is low, typically requiring many months of culturing of virally-transformed (p53/Rb deficient) human cells that have entered telomere crisis [11]. The low frequency of conversion to ALT suggests that mutations and/or infrequent epigenetic alterations are required to unleash this pathway. Indeed, in telomerase-positive mammalian cells with fully functional telomeres, telomeric recombination is stringently repressed by the TRF2, Rap1, and POT1 components of shelterin as well as by the Ku70/80 heterodimer [6,19–23]. Mutations in shelterin and Ku might therefore be anticipated in ALT, a notion that is tested here.

Recently, a subset of pancreatic neuroendocrine tumors (PanNETs) were found to have ultrabright telomeric FISH signals, suggesting the presence of ALT-like long telomeres [24,25]. These tumors also exhibited alterations in ATRX or its binding partner DAXX. Twenty-five PanNETs with ultrabright telomeric foci had *ATRX/DAXX* mutations or lacked nuclear ATRX/DAXX protein. In contrast, 16 PanNETs with apparently normal ATRX/DAXX lacked the aberrant telomeric staining patterns. The same correlation between inactivation of the ATRX pathway and the ALT-like phenotype was observed in pediatric glioblastoma and several other cancers [16,26].

ATRX and DAXX act together in a replication-independent chromatin assembly pathway that deposits the histone variant H3.3 at telomeres and perhaps at other G-rich repetitive elements [27–31]. The function of ATRX/DAXX and histone H3.3 at telomeres is not yet clear, but diminished ATRX function has been documented to increase TTAGGG repeat containing telomeric transcripts (referred to as TERRA [32]), reduce telomeric loading of HP1α, and cause modest levels of telomere dysfunction in mouse ES (but not NIH3T3) cells as gleaned from the localization of γ-H2AX at chromosome ends [29,31]. ATRX deficiency also leads to a defect in sister chromatid cohesion and aberrant mitoses, culminating in the formation of micronuclei, lobulated nuclei, and chromatin bridges [33–35].

Because functional assessment of ALT is not possible in tumor specimens, further tests for the association of ALT with ATRX/DAXX deficiency requires analysis of in vitro immortalized cell lines. Here we describe the results of a comprehensive effort to characterize the genetic alterations and associated phenotypes of 22 human ALT cell lines. We found loss of ATRX in 90% of in vitro immortalized ALT lines, suggesting that inactivation of ATRX is a major step in generating the ALT phenotype. We also document that ALT cell lines are characterized by extensive genomic instability, formation of micronuclei, an aberrant G2/M checkpoint, and abnormal DSB repair kinetics.

Results

Most human ALT cell lines lack ATRX

We assembled a panel of 22 human ALT cell lines (Table 1), nineteen of which originated from in vitro immortalization experiments and four of which were derived from human tumors (three osteosarcomas and one lung adenocarcinoma). Many of the in vitro immortalized lines expressed SV40- or HPV-derived oncoproteins. Seven cell lines originated from a single individual with cystic fibrosis (JFCF-6 series); an additional five cell lines were established from a Li-Fraumeni patient (IIICF series). We confirmed the absence of telomerase activity by TRAP assay (data not shown) and the presence of extra-chromosomal telomeric C-circles, supporting the interpretation that these were ALT cells [8,17] (Table 1; Figure S1).

The ALT cell lines and non-ALT controls (hTERT-immortalized SV40-transformed BJ fibroblasts and the telomerase-positive HPV-E6/E7 expressing HeLa cervical tumor cell line) were tested for the expression of ATRX and DAXX (Figure 1A–1C and data not shown). Repeated immunoblots on independently harvested whole cell extracts indicated that among the 22 ALT cell lines, only six (G292, IIICF-E6E7/C4, IVG-BF.LXN, LFS-05F-24, SK-LU-1, and MeT-4A), contained detectable full length ATRX protein and one of these (IVG-BF.LXN) appeared to lack DAXX. Of the six cell lines expressing ATRX, three (G292, IIICF-E6E7/C4, and IVG-BF.LXN) showed very low immunofluorescence signals for ATRX and/or DAXX (Figure 1B), whereas the other three lines displayed the punctate nuclear staining pattern for ATRX and DAXX expected for this PML body component [36,37]. Thus, 19 out of 22 ALT lines had an alteration in the expression of ATRX and/or DAXX. As each of the seven JFCF-6-derived ALT lines lacked detectable ATRX, we considered the possibility that the parental JFCF-6 culture might have been deficient in ATRX expression. However, a non-ALT JFCF-6 line contained ATRX (Figure 1C), indicating that the lack of ATRX in the other JFCF-6 lines was potentially correlated with the ALT phenotype.

All ALT cell lines were tested for genetic changes in *ATRX*, *DAXX*, and *H3.3* (*H3F3A*) using primers designed to PCR-amplify all exons from these genes for Sanger sequencing (Table 1; Table S1). Failure to amplify multiple consecutive exons was interpreted as a deletion event only when flanking exons did amplify. By that criterion, 6 cell lines (JFCF-6/T.1D, JFCF-6/T.1L, JFCF-6/T.1R, JFCF-6/T.1J/5H, JFCF-6/T.1J/1-3C, and IIICF-T/B3) har-

Table 1. Description of ALT lines used in this study and summary of results.

Cell Line	Tissue Type	Disease (a)	Transformation	C-circles (b)	ATRX protein (c)	ATRX gene (d)	DAXX protein (c)	DAXX gene	H3F3A gene	Micronucleation (e)	G2/M checkpoint initiation (f)	G2/M checkpoint maint (g)	DSB repair (h)	DSB repair (i)	% cells with >10 53BP1 foci (j)	Reference
JFCF-6/T.1D	Jejunal fibroblast	CF	SV40 ER	100*	**undetectable**	**deletion**	normal	wild type	wild type	8±1.4	**27±4**	**69±6**	0.1±5	normal	44	60
JFCF-6/T.1L	Jejunal fibroblast	CF	SV40 ER	303±54	**undetectable**	**deletion**	normal	wild type	wild type	**12±0.9**	**46±5**	**81±4**	*nt*	*nt*	**72**	(k)
JFCF-6/T.1M	Jejunal fibroblast	CF	SV40 ER	76±7	**undetectable**	wild type	normal	wild type	wild type	**16±0.5**	*73±3*	**39±12**	*nt*	*nt*	**62**	(k)
JFCF-6/T.1Q	Jejunal fibroblast	CF	SV40 ER	120±8	**undetectable**	wild type	normal	wild type	wild type	**10±3.9**	**8±18**	**56±19**	**27±2**	**deficient**	51	(k)
JFCF-6/T.1R	Jejunal fibroblast	CF	SV40 ER	42±7	**undetectable**	**deletion**	normal	wild type	wild type	9±3.8	**60±5**	*nt*	**19±15**	**deficient**	53	11
JFCF-6/T.1J/5H	Jejunal fibroblast	CF	SV40 ER	217±57	**undetectable**	**deletion**	normal	wild type	wild type	9±3.9	**4±1**	**64±7**	**14±15**	**deficient**	31	60
JFCF-6/T.1J/1-3C	Jejunal fibroblast	CF	SV40 ER	82±16	**undetectable**	**deletion**	normal	wild type	wild type	**10±1.1**	**1±4**	*nt*	**40±8**	**deficient**	55	38
IIICF/a2	Breast fibroblast	LF	spontaneous	402±44	**undetectable**	wild type	normal	wild type	wild type	**17±5.6**	*60±10*	*nt*	*nt*	*nt*	**88, 87**	11
IIICF/c	Breast fibroblast	LF	spontaneous	125±20	**undetectable**	wild type	normal	wild type	wild type	**14±3.0**	89±1	**58±8**	*nt*	*nt*	**73, 71**	61
IIICF-T/A6	Breast fibroblast	LF	SV40 ER	199±5	**undetectable**	wild type	**undetectable**	wild type	wild type	**11±4.1**	**28±6**	*nt*	*nt*	*nt*	**66, 68**	61
IIICF-T/B3	Breast fibroblast	LF	SV40 ER	278±45	**undetectable**	**deletion**	normal	wild type	wild type	**16±1.3**	82±2	**79±3**	*nt*	*nt*	**74, 78**	61
IIICF-E6E7/C4	Breast fibroblast	LF	HPV	101±24	**abnormal IF**	wild type	normal	wild type	wild type	**24±1.2**	*83±8*	*nt*	*nt*	*nt*	**81, 85**	61
IVG-BF.LXSN	Breast fibroblast	LF	spontaneous	395±89	**abnormal IF**	wild type	**low level/ abnormal IF**	wild type	wild type	**27±3.7**	83±2	*nt*	*nt*	*nt*	**71, 77**	(l)
LFS-05F-24	Skin fibroblast	LF	spontaneous	142±8	normal	wild type	normal	wild type	wild type	**20±5.9**	*77±5*	*nt*	*nt*	*nt*	**68, 73**	8
WI38-VA12/2RA	Fetal lung fibroblast	n/a	SV40	67±11	**undetectable**	wild type	normal	wild type	wild type	7±2.9	*48±10*	**67±5**	**50±11**	**deficient**	21, 37	61
SUSM-1	Embryonic liver fibroblast	n/a	chemical	78±22	**undetectable**	wild type	normal	wild type	wild type	**24±3.6**	*92±1*	*nt*	**41±5**	**deficient**	46, 56	61, 62
GM847	Skin fibroblast	LN	SV40	117±5	**undetectable**	wild type	normal	wild type	wild type	6±1.0	*44±9*	*nt*	**54±5**	**deficient**	17, 38	61
MeT-4A	Pleural mesothelium	n/a	SV40 ER	50±7	normal	wild type	normal	wild type	wild type	**15±6.5**	*nt*	**58±3**	**31±8**	**deficient**	17, 23	61
SaOS-2	Bone	OS	n/a	661±90	**undetectable**	wild type	**low level**	wild type	wild type	**16±4.3**	71±5	*nt*	*nt*	*nt*	**72**	1
G292	Bone	OS	n/a	112±12	**abnormal IF**	wild type	**abnormal IF**	wild type	wild type	**12±1.6**	84±2	**80±7**	**44±14**	**deficient**	22. 22	1

Table 1. Cont.

Cell Line	Tissue Type	Disease (a)	Transformation	C-circles (b)	ATRX protein (c)	ATRX gene (d)	DAXX protein (c)	DAXX gene	H3F3A gene	Micronuclei (e)	G2/M checkpoint initiation (f)	G2/M checkpoint maint (g)	DSB repair (h)	DSB repair (i)	% cells with >10 53BP1 foci (j)	Reference
U-2 OS	Bone	OS	n/a	104±38	**undetectable**	**deletion**	normal	wild type	wild type	7±2.5	95±1	99±1	**33±1**	**deficient**	7, 9	1
SK-LU-1	Bronchial epithelium	Lung adenocarcinoma	n/a	323±31	normal	wild type	normal	wild type	wild type	**16±3.1**	*6±18*	*nt*	*nt*	*nt*	**75**	1

[a]CF, cystic fibrosis; HPV, human papillovirus 16 E6 and E7; LF, Li-Fraumeni syndrome; LN, Lesch-Nyhan syndrome; OS, osteosarcoma; SV40 ER, simian virus 40 early region.
[b]Values are averages of triplicate assays (±SD) with JFCF-6/T.1D set to 100 in each assay and the other values expressed relative to this standard. BJ and HeLa values are below 2.
[c]Bold: aberrant ATRX or DAXX protein in western and/or IF. ATRX western results are from three independent immunoblots. Examples of abnormal IF are given in Figure 1b.
[d]Bold: deletions in ATRX. See Table S1 for details.
[e]Values represent mean % cells with micronuclei and SDs from three independent experiments. See Figure 4. Values for HeLa and BJ/SV40 are <8%. Bold: >10% of cells with micronuclei.
[f]Bold: abnormal G2/M checkpoint initiation (<70% reduction in mitotic index 1 hr after 10 Gy IR). See Figure 5A. Italic: uninterpretable due to low mitotic index. hTERT-RPE (positive control) 89% and ATM-/- GM5849 46%.
[g]Bold: abnormal G2/M checkpoint maintenance (<90% reduction in mitotic index 16 hr after 4.5 Gy IR). See Figure 5b. Italic: low mitotic index at 16 hr in noc. Values for HeLa and BJ/SV40 were 98±2% and 96±3%, respectively.
[h]Bold: slow DSB repair kinetics. See Figure 6A and Figure S8. After 0.5 Gy IR, cells with >10 53BP1 foci were scored at 1 and 24 hr and without IR. Values represent (% at 24 hr)-(% no IR)/(% at 1 hr)-(% no IR). nt: not tested.
[i]Bold: abnormal residual DNA fragmentation 24 hr post IR. See Figure 6B. nt: not tested.
[j]Bold: greater than 60% of cells containing >10 spontaneous 53BP1 foci.
[k]A. Englezou, P. Bonnefin, R. Reddel, unpublished data.
[l]J. Plowman, L. Huschtscha, R. Reddel, unpublished data.
doi:10.1371/journal.pgen.1002772.t001

bored large deletions in the *ATRX* gene that ranged from 4 to 26 exons in size (Table 1; Table S1).

Sequencing of genes that did not harbor detectable deletions revealed no potentially inactivating genetic changes. Nine of those cell lines lacked detectable ATRX protein suggesting that genetic alterations not detectable by Sanger sequencing, such as translocations, promoter or splicing mutations, or epigenetic changes may underlie their lack of expression. No genetic alterations were detected in *DAXX* or the *H3F3A* gene encoding H3.3 (Table 1).

These data provide strong evidence that loss of ATRX expression is involved in either the initiation or maintenance of the ALT pathway in human cells. To test whether deficiency in ATRX was sufficient to induce the telomere-telomere recombination typical of ALT cells, we used an shRNA to deplete ATRX from HeLa cells and used Chromosome-Orientation FISH (CO-FISH) to measure sequence exchanges between sister telomeres (Telomere Sister Chromatid Exchanges or T-SCEs). Despite repression of ATRX by more than 95%, the frequency of T-SCEs was not significantly altered (Figure 1D and 1E). In addition, repression of ATRX or DAXX in SV40-transformed BJ fibroblasts failed to induce escape from crisis (Figure 1F and 1G; Figure S2), whereas expression of hTERT readily immortalized the cells (Figure 1G; Figure S2). After a prolonged period in crisis (6 weeks), immortal clones emerged from the culture in which ATRX expression was suppressed with ATRX sh590. However, a parallel culture in which ATRX was not suppressed efficiently (ATRX sh589) also yielded an immortal subpopulation (Figure 1F and 1G) and in both cases, the immortal cells expressed telomerase and lacked telomeric C-circles (Figure S2A and S2B), indicating that they had not activated ALT. These observations argue that this level of ATRX/DAXX suppression is not sufficient to activate the ALT pathway.

No overt changes in shelterin or 299 potentially ALT relevant genes

The lack of induction of ALT by shRNA-mediated suppression of ATRX and DAXX prompted us to inspect the ALT cell line panel for changes in the status of genes, pathways, and proteins with possible relevance to the activation of ALT. Because HDR is normally repressed at telomeres by shelterin, we examined the expression of all six shelterin components in the ALT lines by repeated immunoblotting (Figure S3). Using this approach on all 22 ALT lines failed to reveal a consistent change in the abundance or appearance of the six shelterin proteins. In addition, exome sequencing (see below) failed to reveal mutations in the genes encoding TRF1, TRF2, Rap1, POT1, TIN2, and TPP1.

A second entity associated with telomeres is the telomeric RNA, TERRA [32]. As mouse ATRX deficient cells were reported to have elevated TERRA levels and selected ALT cells were previously found to have higher levels of TERRA [31,38], we examined the expression of this RNA in the ALT lines. Quantitative Northern analysis confirmed that the ALT lines generally have higher TERRA levels than telomerase-positive cells, but some ALT lines (e.g. JFCF-6/T.1D and IIICF-E6E7/C4) approximated the levels of TERRA found in BJ/hTERT/SV40 and HeLa cells (Figure S4). There was no clear correlation between increased TERRA and ATRX status since the cell lines with apparently normal ATRX/DAXX (LFS-05F-24, SK-LU-1, and MeT-4A) had TERRA levels comparable to, or higher than, cell lines lacking ATRX (e.g. JFCF-6/T.1D, JFCF-6/T.1R, and JFCF-6/T.1L) (Figure S4).

In addition to shelterin and TERRA, we analyzed 299 genes with potential relevance to telomeres and the ALT pathway. This gene set included genes encoding proteins involved in telomere

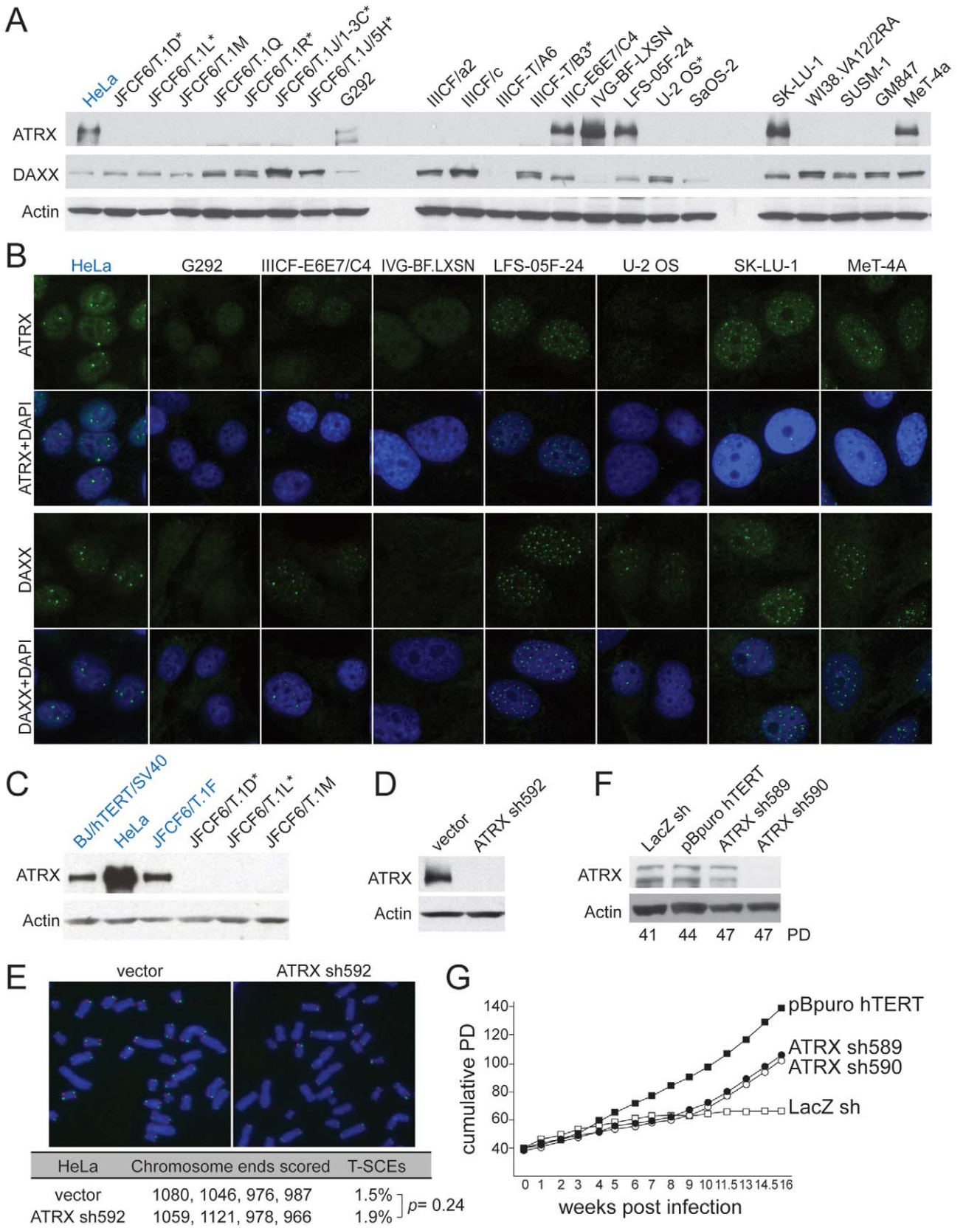

Figure 1. Deficiency in ATRX/DAXX correlates with ALT. A, Immunoblot for ATRX and DAXX in the indicated ALT lines. ATRX was detected with A301-045 (Bethyl Labs). DAXX was detected with A301-353A (Bethyl Labs). Asterisk: cell lines with deletions in the *ATRX* gene (see Table 1 and Table S2). HeLa cells (blue) were used as a positive control. B, IF for ATRX and DAXX in the indicated cell lines. HeLa cells (blue) are used as a positive control. C, Immunoblot for ATRX in additional non-ALT, positive control cells (blue) relative to the indicated ALT lines. D, Immunoblot showing >90%

reduction of ATRX protein in HeLa cells expressing ATRX shRNA592. E, T-SCEs, a measure for telomeric recombination, assessed by Chromosome Orientation (CO)-FISH on metaphases harvested from HeLa cells expressing vector or ATRX shRNA592. The average percentage of T-SCEs from four independent experiments is shown, with a *p* value derived from a two-tailed, unpaired *t* test. F, Immunoblot showing >90% reduction of ATRX protein in cells expressing ATRX shRNA590 but not with shRNA589. G, Growth curves showing immortalization of SV40-transformed BJ fibroblasts infected with an hTERT expressing retrovirus but no immortalization after infection with the effective (sh590) and ineffective (sh589) shRNAs to ATRX.
doi:10.1371/journal.pgen.1002772.g001

maintenance, DNA damage repair and signaling, chromosome duplication and segregation, and cell cycle regulation (Table S2). The coding regions of these genes were analyzed by massively parallel 454 sequencing on genomic DNA derived from 14 of the 22 ALT lines. We focused on ALT lines generated *in vitro* as opposed to tumor-derived ALT lines to exclude genetic changes selected for during tumorigenesis. The JFCF-6 and IIICF ALT lines are derived from two individuals, allowing identification of SNPs specific to the individual as well as potential ALT-correlated changes. After excluding known SNPs, the remaining sequence data were filtered to exclude apparent SNPs present in less than 25% of the reads. The rare SNPs that eluded the threshold filter affected 20 genes (Table S3). Within the JFCF-6 and IIICF cell line sets, a nucleotide change in multiple members of either set was interpreted as being present prior to the acquisition of the ALT phenotype, and thus not relevant. The variable occurrence of these SNPs in the multiple ALT lines derived from one individual (e.g. only two of the five IIICF derived lines have the BLM K323R) is likely due to chromosome losses occurring during or after telomere crisis. The florid chromosome instability exhibited by these cell lines (see below) makes this an appealing and parsimonious explanation. Some of these SNPs were also found in other cell lines (e.g. MDC1 C1559G in LSF-05F-24 and IVG-BF.LXSN) and deemed irrelevant based on their presence in the IIICF and/or JFCF-6 lines prior to the induction of ALT. Based on these criteria, no ALT specific change was observed in the five IIICF-derived ALT lines or in IVG-BF.LXN. Three of the JFCF-6 derived ALT lines had a specific change that could not be attributed to a pre-existing SNP (A436S in Suv420H2, S553F/S470F in PRMT5, and D2579V in Ki67; Table S3). Since these genes were not affected in the other 13 ALT lines analyzed, they are unlikely to be critical to ALT. Similarly, LSF-05F-24 contained changes in five genes that are not affected in the other 13 cell lines. Since none of these alterations were found in a substantive fraction of the ALT cell lines, it is unlikely that these genes represent clear contributors to the ALT phenotype.

Extensive genome rearrangements in ALT

As ALT-relevant genetic alterations might be identified from recurrent regions of gene copy number changes, we analyzed the ALT cell line panel using Affymetrix 6.0 single nucleotide polymorphism (SNP) arrays to identify regions of recurrent copy number alteration. When we examined either individual cells (Figure 2A and 2B) or the entire set as a group (GISTIC analysis, Figure S5), we found that the number and complexity of these gains and losses were at least as extensive as the alterations in human cancers with genome instability [39]. When we considered all of the ALT cell lines as a group, we identified 18 regions of significant focal copy number gain, and many more regions of copy number loss (Figure S5).

The genome rearrangements in the ALT lines are a likely consequence of the telomere dysfunction these cells experienced prior to their immortalization. Consistent with this idea, SKY analysis of five ALT lines (JFCF-6/T.1R, JFCF-6/T.1Q, IVG-BF.LXN, IIICF/c, and LFS-05F-24) showed frequent non-reciprocal translocations, deletions, complex rearrangements, and hyper-triploid chromosome numbers (Figure 3), all of which can be caused by telomere dysfunction [40,41]. Previous cytogenetic analysis of two ALT cell lines (Saos-2 and ZK-58) also indicated frequent translocations, deletions, and complex rearrangements [42].

In cells that have been immortalized by telomerase activation, the telomere-driven genome instability is largely dampened, resulting in a rearranged but now relatively stable karyotype [43,44]. We asked whether ALT similarly stabilizes the genome by examining two generations of clonal descendants of the JFCF-6/T.1R ALT line. Although the clones exhibited features in common with the parental cell line, each of the clones showed new regions of copy number gain or loss (Figure 2B). For instance, a new gain of a segment on chromosome 2q was observed in one single cell clone of the parental line (and all the clones derived from it), and in another clone (and its derivatives) an overlapping segment showed a new deletion. Many other changes, including examples on chromosomes 6, 12, 14, 15, 16 and 21, showed obvious new gains or losses as compared to the parental clone, with independent clones showing different alterations. In contrast, we found only rare clonal alterations in single cell clones derived from the telomerase-expressing HCT116 cell line. These observations suggest that the JFCF-6/T.1R and perhaps other ALT lines have ongoing genome instability as well as highly rearranged genomes.

We considered that ongoing genome instability in the ALT lines could be due to defects in mitosis and/or dicentric chromosomes resulting from telomere dysfunction and ATRX deficiency. Defects in mitosis and dicentric chromosomes can give rise to lagging chromosomes that can form micronuclei, which were recently shown to engender massive genomic alterations [45]. We therefore examined the ALT lines for the spontaneous occurrence of micronuclei. Fifteen of the 22 ALT lines showed a high frequency (10–30%) of cells with micronuclei (Table 1; Figure 4A and 4B). As expected, SV40-transformed hTERT-expressing BJ fibroblasts and HeLa cells showed the low level of spontaneous micronucleation (<8%) previously noted in other transformed human cells [46]. Micronucleation frequencies of up to 15% were previously only observed in cells experiencing high levels of DNA damage ensuing from γ-irradiation, in genetic contexts associated with high levels of spontaneous DNA damage, and in genomically unstable tumor cell lines (e.g. [47,48]; Neill Ganem and David Pellman, pers. comm.). Thus, many ALT cell lines show an unusually high frequency of micronucleation, indicative of ongoing genome instability. The micronucleation phenotype of ALT lines is likely to be in part due to the absence of ATRX since depletion of ATRX with two shRNAs induced the formation of micronuclei in BJ/hTERT/SV40 and HeLa cells (Figure 4C and 4D), consistent with a previous report on the induction of lobulated nuclei after ATRX depletion [35].

G2/M checkpoint function and DSB repair kinetics in ALT lines

The signs of ongoing genome instability in ALT cells led us to examine the functionality of DNA damage checkpoints and DSB repair. As the ALT lines were expected to have an impaired G1/S DNA damage checkpoint due to their p53 deficiency, we focused our efforts on the G2/M checkpoint. Entry into mitosis is blocked upon activation of the ATM and/or ATR signaling pathways.

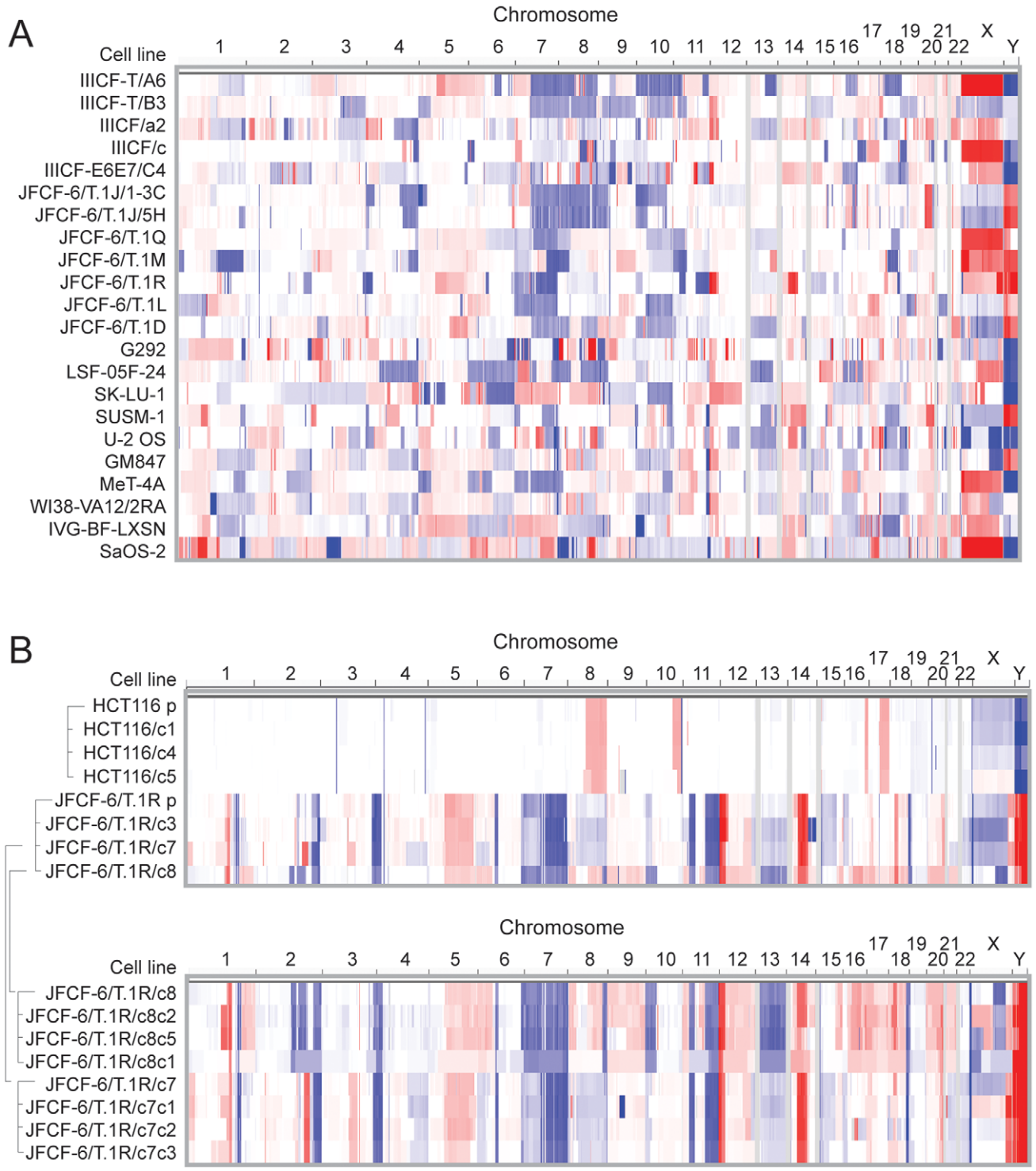

Figure 2. Copy number analysis showing extensive genome rearrangements in ALT lines. SNP array copy number results are shown for (A) the ALT cell lines and (B) the 1st and 2nd generation subclones derived from JFCF-6/T.1R (indicated by the brackets) and subclones derived from the telomerase-positive HCT116 control. Segmented copy number data is shown for each chromosome, by genomic position in columns and by cell line in rows. The color scale ranges from red (amplification; log2 copy number ratio of 1.5) through white (neutral; 2 copies in diploid lines, log2 ratio of 0) to blue (deletion; log2 ratio of −1.5).
doi:10.1371/journal.pgen.1002772.g002

ATM signaling is primarily responsible for the initiation of the checkpoint, whereas ATR signaling ensures the maintenance of the arrest [49]. To determine the efficiency of initiation and maintenance of the G2/M checkpoint, subconfluent cells were subjected to ionizing radiation, and the mitotic index was determined by flow cytometric quantitation of histone H3 (S10) phosphorylation. One hour after treatment with 10 Gy ionizing radiation (IR), the mitotic index of control hTERT-immortalized

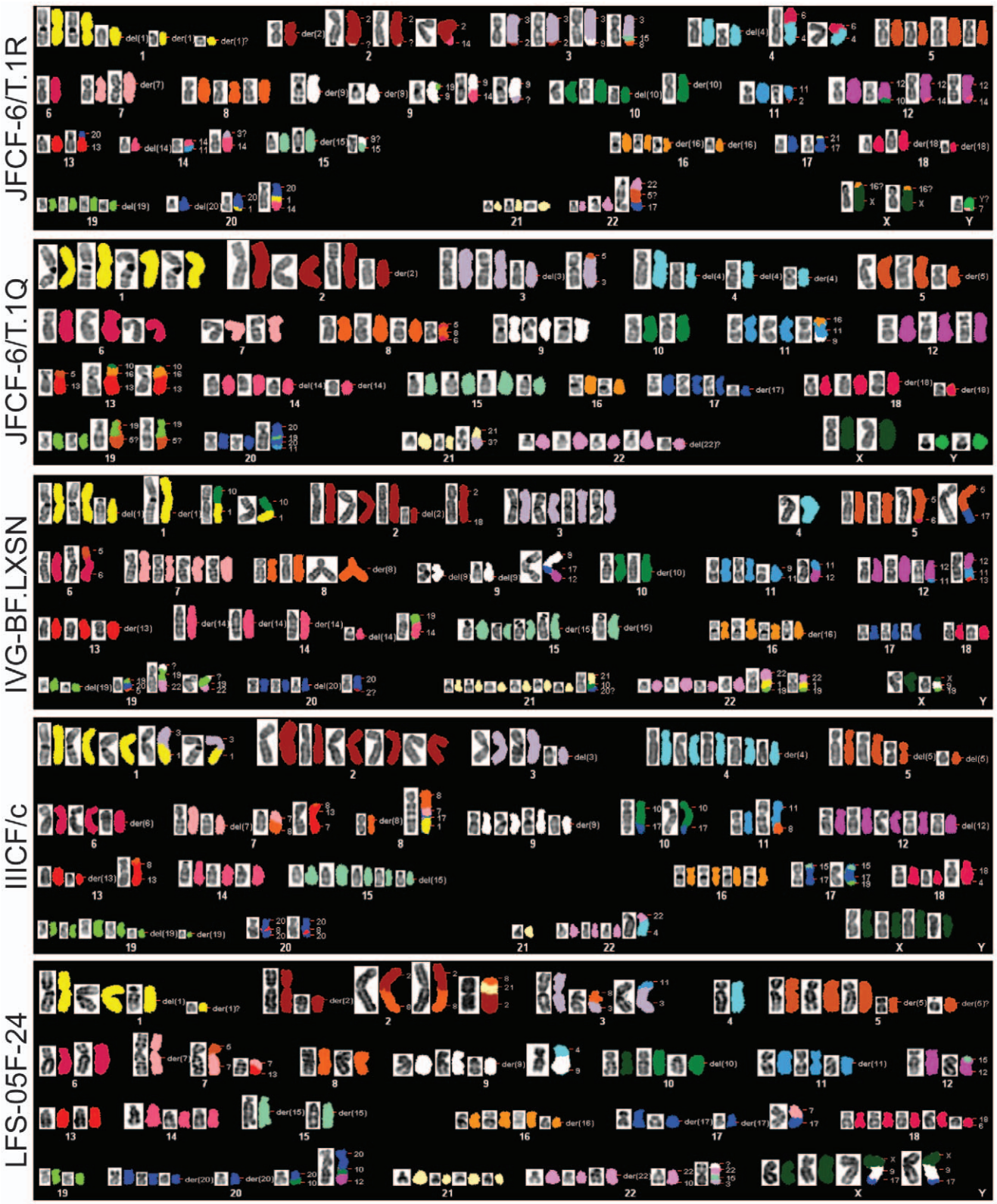

Figure 3. Abnormal karyotypes in ALT lines. Representative metaphases from 5 cell lines showing subtetraploid karyotype with high number of rearranged chromosomes (up to 60%). Structural rearrangements are labeled as following: del(Z)- deletion of chromosome Z; der(Z) - multiple aberrations within single chromosome Z; chromosome, denoted with two or more numbers indicate rearrangement involving two or more partners.
doi:10.1371/journal.pgen.1002772.g003

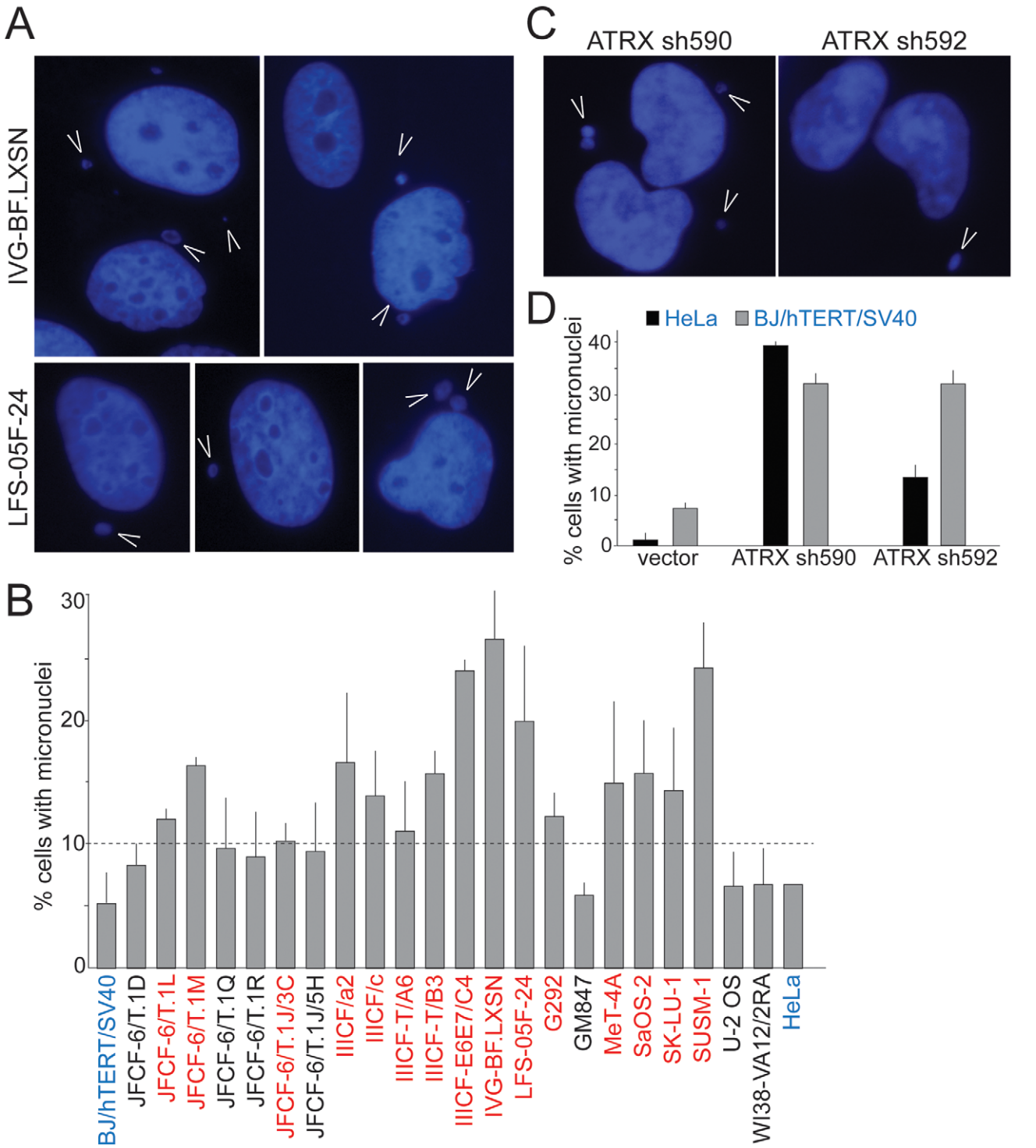

Figure 4. Frequent micronucleation in ALT cells may be attributable to loss of ATRX. A, Examples of micronuclei (arrowheads) in two ALT cell lines. Blue: DAPI stain for DNA. B, Graph showing micronucleation frequencies in the ALT cell lines and two telomerase positive controls (blue). Values are means ±SD from three experiments (>100 nuclei each). Red: cell lines with >10% micronucleation frequency (dashed line). HeLa cells were analyzed once. C, Examples of micronuclei (arrowheads) in HeLa cells expressing two independent ATRX shRNAs (see Figure 1 for immunoblots). D, Graph showing micronucleation frequencies in two telomerase positive cell lines infected with vector or the indicated ATRX shRNAs. Values are means ±SEM from two experiments (200 nuclei each).
doi:10.1371/journal.pgen.1002772.g004

Retinal Pigment Epithelial cells (RPE/hTERT) was reduced approximately ten-fold (from 2.7% to 0.3%), whereas reduction in the mitotic index of ATM-deficient GM5849 cells was less than two-fold (from 4.1% to 2.3%) (Table 1; Figure 5A). Of fourteen ALT lines that had a sufficiently high mitotic index to yield interpretable results, half showed a severe defect in G2/M

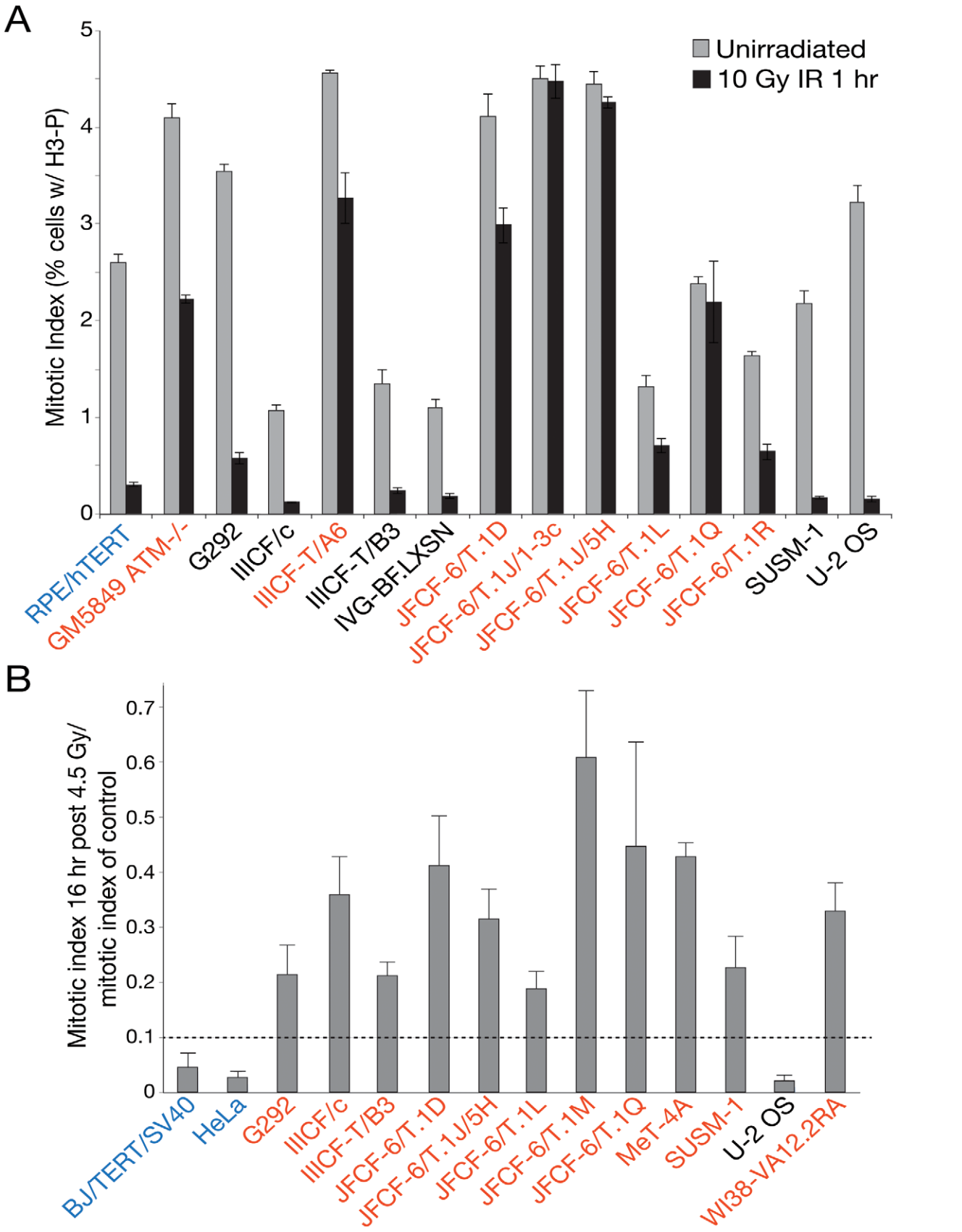

Figure 5. Many ALT lines have a defect in the G2/M checkpoint initiation and/or maintenance. A, Bar graph depicting the results of an assay for the initiation of the G2/M checkpoint at 1 hr after irradiation of the indicated cell lines. RPE/hTERT is a positive control (in blue). Mean ± SD

for triplicate experiments are shown. B, Bar graph depicting the results of an assay for the maintenance of the G2/M checkpoint at 16 hr after IR. BJ/hTERT/SV40 is a positive control (in blue). Mean ± SD for triplicate experiments are shown. See Table 1 for summary. Cell lines in red have a defect in the G2/M checkpoint.
doi:10.1371/journal.pgen.1002772.g005

checkpoint initiation (Figure 5A; Table 1). In six ALT lines, the checkpoint defect was more severe than that of ATM-deficient cells. Qualitatively similar results were observed in response to low dose (1 Gy) IR treatment, with the same cell lines exhibiting defects as at the high dose (data not shown). Similarly, 10 of 11 ALT lines tested displayed a deficiency in the maintenance of the G2/M checkpoint, monitored at 16 hr after γ-irradiation with 4.5 Gy (Table 1; Figure 5B). Some of the ALT lines were proficient in the initiation of the checkpoint but failed to maintain it (e.g., IIICF/c). Collectively, we observed impaired G2/M checkpoint function in 11 out of 17 ALT lines tested. This defect in the G2/M checkpoint is not seen in established non-ALT human cell lines.

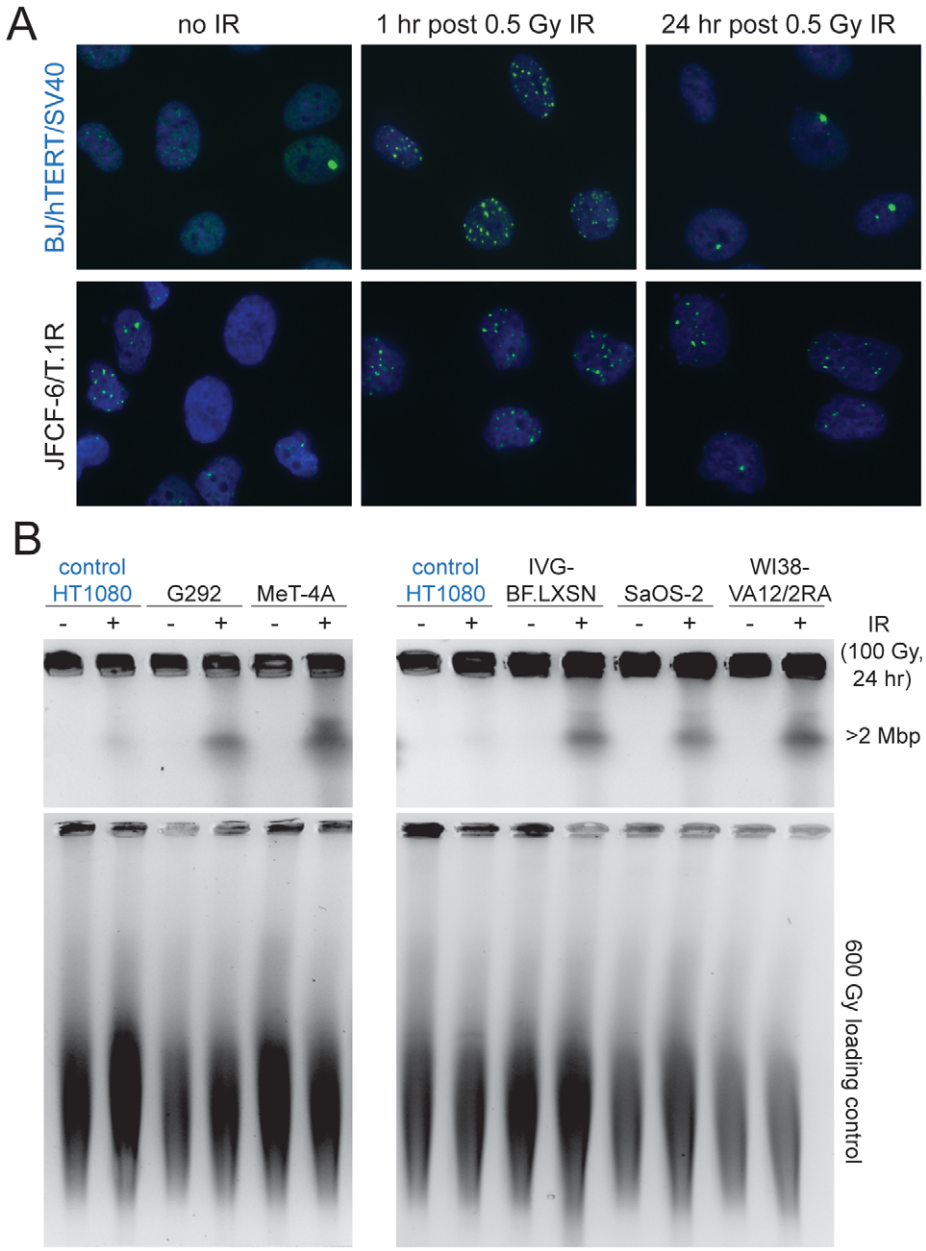

Figure 6. Deficiency in DSB repair in ALT lines. A, Example of assay for 53BP1 foci in the positive control (BJ/hTERT/SV40, blue) (top) and an ALT line (bottom). Cells were treated as indicated above the panels and stained for DNA with DAPI (blue) in conjunction with IF for 53BP1 (green). Note the higher level of 53BP1 foci in non-irradiated ALT cells and incomplete DSB repair at 24 hr after IR. B, Example of PFGE-assay for DSB repair in the indicated cell lines. Cells were treated with 100 Gy IR 24 hr before harvesting and residual DSBs were evaluated based on the DNA fragments released from agarose embedded cells into a PFGE gel. Plugs were treated with 600 Gy to fragment the DNA and run in parallel to serve as a control for loading. DNA was stained with ethidium bromide after electrophoresis. HT1080 (fibrosarcoma cell line) was used as a positive control (in blue).
doi:10.1371/journal.pgen.1002772.g006

For example, normal G2/M arrest following γ-irradiation is observed in HT1080, HCT116, IMR90 (JHJP, unpubl. data), 293T [50], MCF7, and genetically complemented HCC1937 cells [51]. The decrement in the G2/M checkpoint did not reflect a global impairment of DNA damage response (DDR) signaling in the ALT cells, since phosphorylation of CHK2, an outcome of ATM signaling, was readily apparent upon IR treatment in all cell lines, but undetectable in GM5849 (ATM-deficient) cells (Figure S6). Indeed, CHK2 phosphorylation was evident in several of the ALT cell lines prior to irradiation, consistent with the finding that the ALT phenotype is associated with chronic genotoxic stress (Figure S6).

In addition to an abnormal G2/M checkpoint, many of the ALT cell lines showed unusually slow DSB repair kinetics. To assay this aspect of the DDR, cells were γ-irradiated with 0.5 Gy and the fraction of cells with 10 or more 53BP1 foci was scored after 1 and 24 hr as well as in non-irradiated controls (Figure 6A; Figure S7; Table 1). As expected, non-ALT cell lines (HeLa and hTERT immortalized SV40-transformed BJ) showed a nearly complete disappearance of the IR-induced DNA damage foci at 24 hr. In contrast, 11 out of 12 ALT cell lines retained a significant fraction of the induced 53BP1 DNA damage foci after a day (Table 1; Figure 6A). This result was corroborated with a pulsed field gel electrophoresis (PFGE)-based gel assay for the disappearance of IR-induced DNA fragmentation after 24 hr (Figure 6B; Table 1). We also noted that approximately half of the ALT cell lines had a high basal level of cells containing 10 or more 53BP1 foci, further confirming that ALT cells experience ongoing genome damage (Table 1). These spontaneous 53BP1 foci could be the result of both genome-wide DNA breaks and the presence of dysfunctional telomeres [52]. Their deficiency in the G2/M checkpoint, combined with the absence of a functional p53 pathway likely explains why these cells proliferate despite severe genome damage.

Discussion

Here we report that ATRX is either undetectable or severely depleted from PML bodies in ~90% of human ALT cell lines tested, including ALT lines derived in vitro. This result establishes a strong correlation between the initiation or maintenance of ALT and deficiency in the ATRX/DAXX pathway. In a subset of cases, the loss of ATRX is due to large deletions within the ATRX gene, further underscoring the relevance of ATRX status to ALT. We expect that alterations in ATRX/DAXX in cells and tumors will be a useful indicator of the presence of the ALT pathway. However, manipulating ATRX/DAXX expression failed to unleash ALT, suggesting that deficiency of these proteins is not sufficient for the ALT phenotype and pointing to the need to identify the cooperating (epi-) genetic changes. In addition, a key issue for further investigation is the mechanism by which the loss of ATRX/DAXX and concomitant lack of deposition of H3.3 into telomeric chromatin might allow or promote telomere recombination. We note that it remains possible that the ATRX/DAXX pathway has an indirect effect, for instance by repressing genes that promote telomere recombination.

Our data have uncovered a hitherto unappreciated level of genome instability in ALT cells. All ALT lines, including cell lines that arose from in vitro immortalization experiments, harbor scrambled genomes and have signs of ongoing genome instability. The ALT lines have frequent micronuclei, a high basal level of DNA damage foci, and elevated checkpoint signaling in absence of exogenous damage. Furthermore, in one ALT cell line, repeated subcloning established frequent copy number alterations. These features of ALT raise the possibility that tumors employing this pathway will have unique vulnerabilities that could offer clinical utility, such as has been shown for cells lacking BRCA1 that are sensitive to PARP inhibition [53]. This possibility underscores the importance of establishing a signature for the ALT phenotype.

In this context, it is notable that G2/M checkpoint deficiency emerged as a prominent attribute of many ALT cells in this study. It is likely that the diminished G2/M checkpoint response allows these cells to proliferate, despite a considerable burden of DNA damage both at telomeres and elsewhere in the genome. G2/M checkpoint deficiency is an example of a potential vulnerability unique to ALT cells. Indeed, G2/M checkpoint inhibitors to enhance efficacy of clastogenic therapies are currently being developed and evaluated in clinical trials [54].

The altered G2/M response could not be ascribed to mutations in known components of the ATM or ATR signaling pathways. Furthermore, DNA damage signaling was demonstrably intact since CHK2 phosphorylation could be induced by exogenous DNA damage. The implication of ATRX and DAXX in the ALT phenotype may have some relevance to the checkpoint defects observed, as the involvement of chromatin remodelers in the DDR becomes increasingly clear [55]. Nevertheless, identification of the mechanisms underlying G2/M checkpoint dysfunction in ALT cells is warranted given the data presented here.

Our results would appear to exclude the possibility that the ALT cells arise from a single dominant mutation in addition to p53/Rb loss. Loss of ATRX/DAXX function appears to be required for ALT but it seems likely that a defect in the G2/M checkpoint is also needed in order for the cells to proliferate, given their high level of spontaneous DNA damage. The view that multiple steps are required to allow ALT-mediated immortalization is consistent with the low frequency by which it arises, even in SV40- or HPV-transformed cells.

Materials and Methods

Cell lines

ATL cell lines are described in Table 1. CellBank Australia provided cell line quality control. All cell lines were verified by 16-locus STR profiling and confirmed to be free of Mycoplasma species, or were analyzed within 10 population doublings of being obtained from ATCC. Non-ALT cell lines were obtained from the ATCC. The HeLa cell line (subclone HeLa1.3) was described previously [56].

Sequence analysis of *ATRX*, *DAXX*, and *H3.3* genes

Primers were synthesized by Invitrogen (San Diego, CA) to cover all exons of *ATRX*, *DAXX*, and *H3F3A1* (H3.3). PCR was performed in 5 μl reactions containing 1× PCR Buffer (67 mM Tris-HCl, pH 8.8, 6.7 mM MgCl2, 16.6 mM NH4SO4, 10 mM 2-mercaptoethanol), 1 mM dNTPs (Invitrogen, San Diego, CA), 1 μM forward and 1 μM reverse primers, 6% DMSO, 2 mM ATP,0.25 U Platinum *Taq* (Invitrogen, San Diego, CA) and 3 ng DNA. Reactions were carried out in 384-well ABI 9700 thermocyclers (Applied Biosystems, Foster City, CA) using a touchdown PCR protocol: 1 cycle of 96°C for 2 min; 3 cycles of 96°C for 10 sec, 64°C for 10 sec, 70°C for 30 sec; 3 cycles of 96°C for 10 sec, 61°C for 10 sec, 70°C for 30 sec; 3 cycles of 96°C for 10 sec, 58°C for 10 sec, 70°C for 30 sec; 41 cycles of 96°C for 10 sec, 57°C for 10 sec, 70°C for 30 sec; 1cycle of 70°C for 5 min. The PCR products were evaluated for presence and size by electrophoresis on 2% agarose gels and sequenced as described (refs. 25 and 57 [25,57]). All failed PCRs were repeated at least two more times.

Targeted sequencing of candidate ALT genes

Coding regions of 299 genes were amplified from genomic DNA of 15 samples. Following PCR amplification, products were normalized and pooled prior to emulsion PCR amplification of single stranded DNA and 454 pyrosequencing. Sequencing was performed using a FLX Titanium machine at Agencourt Bioscience Corp. (Beverly MA), to a depth of 20× coverage per sample per amplicon (attempted). Assembly and mapping of reads was performed using AVA software.

Immunoblotting

Immunoblotting was performed using standard procedures on whole cell extracts. ATRX was detected primarily with A301-045 (Bethyl Labs) or with HPA001906 (Sigma Aldrich). DAXX was detected with A301-353A (Bethyl Labs). Immunoblotting for CHK2-P was done with CHK2-T69 (Cell Signaling) and total CHK2 was detected with clone 7 Ab (Millipore). Shelterin components were analyzed as described previously [56].

Immunofluorescence

Cells grown on glass coverslips were fixed with 3% paraformaldehyde for 10 min at room temperature, washed three times with PBS, and permeabilized with 0.5% Triton X-100 in PBS for 10 min on ice. Cells were then washed four times with PBS and blocked for 30 min at room temperature with PBG (0.2% cold water fish gelatin (Sigma), 0.5% BSA, in PBS). Primary antibodies recognizing ATRX and DAXX (Bethyl Laboratories, Inc., see above) were diluted in PBG and incubated on cells for 1.5 h at 37°C. Following three washes with PBG, cells were incubated with FITC-conjugated donkey anti-rabbit secondary antibody (Life Technologies), diluted in PBG, for 30 min at 37°C. Cells were washed three times with PBS and counterstained with 4′,6′-diamidino-2-phenylindole (DAPI).

Quantitative RT–PCR

RNA was extracted from cell lines using the RNeasy kit (Qiagen). 0.5 µg of RNA was reverse transcribed using RT-Advantage kit (Clontech) in a volume of 20 µl according to the manufactures instructions. Following reverse transcription 180 µl of water was added and 5 µl was used for qPCR with specific primers and SYBR green mix (Applied Biosystems). Primers: DAXX 5′: AGACGGTTTCTGAGCATCATC; DAXX 3′: AGAGGAGCTAGGGGCTTCTG; TERT 5′: GCCTTCAAGAGCCACGTC; TERT 3′: CCACGAACTGTCGCATGT.

Analysis of copy number alterations

Affymetrix 6.0 SNP data were generated at the Broad Institute for 22 ALT cell lines and 6 single cell ALT (JFCF-6/T.1R) and non-ALT (HCT116) cell line clones. Single cell clones were generated by fluorescence activated cell sorting (FACS) sorting into 96 well plates. Normalized copy number estimates (log2 ratios) were made and segmented by the Circular Binary Segmentation algorithm as previously described [58]. The GISTIC 2.0 algorithm was performed as previously described on the resulting segmented copy number data from the 22 ALT lines [39,59]. The boundaries of the peak amplified and deleted regions identified by GISTIC 2.0 were set with at least 95% confidence to include the target gene(s).

Functional analysis of DAXX and ATRX

SV40-transformed BJ fibroblasts at PD 38 were infected with either *ATRX*- or *DAXX*-specific shRNAs (Sigma) with the following target sequences: ATRXsh589: GCAGATTGATATGAGAGGAAT; ATRXsh590: CGACAGAAACTAACCCTGTAA; ATRXsh592: CCGGTGGTGAACATAAGAAAT; DAXXsh800 : GAAGGGATGGACTAAGCTAAT; DAXXsh801: TCACCATCGTTACTGTCAGAA; DAXXsh802: GCCACACAATGCGATCCAGAA. LacZ-specific shRNA was used as negative control, while infection with hTERT was used as a positive control. Cells were selected with puromycin (0.5 µg/ml) for 2 days, and at least 10^6 cells of each sub-line were maintained in culture for 110 days. Cultures were split at <80% confluence, and growth medium was replaced every 3 days. Cells were counted at each passage and cumulative PDs were recorded. The suppression of *ATRX* in HeLa1.3 cells was achieved with ATRXsh592.

T-SCE assay for Telomeric Recombination

Cells were grown in 10 µM BrdU:BrdC (3:1) for 16 hr with the addition of 0.1 µg/ml colcemid (Roche) for the final 2 h. Slides were treated with 0.5 mg/ml RNAse A for 10 min at 37°C, stained with 0.5 µg/ml Hoechst 33258 in 2× SSC for 15 min at room temperature, and exposed to 365-nm UV light (Stratalinker 1800 UV irradiator, 5400 J/m^2). Following digestion with Exonuclease III (Promega, 10 U/µl, 2×10 min) at room temperature, slides were dehydrated through an ethanol series (70%, 90%, 100%) and incubated sequentially with TAMRA-TelG 5′-$[TTAGGG]_3$-3′ and FITC-TelC 5′-$[CCCTAA]_3$-3′ probes at room temperature. The percentage of chromosome ends displaying telomeric sister chromatid exchanges (T-SCEs) was calculated from four independent experiments.

SKY

Cells were treated with colcemid for 1 hr, harvested, pelleted, re-suspended in a hypotonic solution of 0.075 M KCl for 18 min, fixed in Carnoy's fixative (3:1 methanol:glacial acetic acid), and washed four times with Carnoy's fixative. All fixed samples were spread on slides for staining or hybridization. Chromosomes were stained with Giemsa or Hoechst to visualize chromosomal abnormalities. Spectral karyotyping (SKY) was performed on mitotic samples according to the SkyPaint DNA kit H-5 for human chromosomes procedure (Applied Spectral Imaging, SKY000029) and imaged on a Nikon Eclipse E6000 microscope equipped with the SD300 Spectracube and Spectral Imaging acquisition software.

G2/M checkpoint analysis

To assess G2/M checkpoint initiation, subconfluent cells were exposed to γ-irradiation and harvested at 1 hr with non-irradiated cells for mitotic index measurement by flow cytometry. Briefly, cell pellets were fixed in 70% ethanol, washed twice with cold PBS, and permeabilized with 0.25% Triton X-100 in PBS for 15 min on ice. Cells were then rinsed with PBS containing 1% BSA and stained with anti-phospho-histone H3 S10 antibody (Cell Signaling) for 1.5 hr at room temperature. Following two washes with PBS containing 1% BSA, cells were stained with a FITC-conjugated donkey anti-mouse secondary antibody (Life Technologies) for 30 min at room temperature. Cells were washed twice with PBS and then stained with propidium iodide (25 µg/ml) in the presence of 0.1 mg/ml RNase. Flow cytometry was performed on a BD Biosciences FACSCalibur, and the percentage of mitotic cells was determined as those that were FITC-positive and contained 4N DNA content. To assess maintenance of the G2/M checkpoint, nocodazole (1 µg/ml) was added 1 hr after irradiation, and cells were incubated at 37°C for 16 hr. Cells were then harvested and processed as described above. To account for differences in the rate of cell cycle progression between cell lines,

the mitotic index of irradiated cells was normalized to that of non-irradiated cells treated with nocodazole for 16 hr.

Micronucleation

Asynchronously growing cells were fixed and examined for the presence of micronuclei after DAPI staining for DNA. Data were obtained from three independent experiments with >100 nuclei examined in each.

C-circle assay

For the C-circle assay, DNA from cell lines was isolated using the DNeasy Blood and Tissue Qiagen kit, digested with *Hinf*I and *Rsa*I, and quantified using Hoechst fluorimetric analysis. DNAs were diluted to approximately 3 ng/µl, quantified again, and the dilutions were adjusted to exactly 3 ng/µl. The assay was performed using 30 ng of quantified DNA as described by Henson et al. [8] using dot-blotting with an end-labeled [AACCCT]4 telomeric oligonucleotide probe. C-circle values in Table 1 were derived from three independent DNA preparations for each cell line.

DSB repair assays

Cells grown on glass coverslips were irradiated with 0.5 Gy IR and incubated at 37°C for 1 hr or 24 hr. Irradiated and non-irradiated cells were fixed with 3% paraformaldehyde for 10 min at room temperature, washed three times with PBS, and permeabilized with 0.5% Triton X-100 for 10 min on ice. Cells were then washed four times with PBS and blocked for 30 min at room temperature with PBG (0.2% cold water fish gelatin (Sigma), 0.5% BSA, in PBS). Primary 53BP1 (Novus) antibody was diluted in PBG and incubated on cells for 1 hr at 37°C. Following three washes with PBG, cells were incubated with FITC-conjugated donkey anti-rabbit secondary antibodies (Life Technologies), diluted in PBG for 30 min at 37°C. Cells were washed three times with PBS and counterstained with 4′,6′-diamidino-2-phenylindole (DAPI). The percentage of cells containing >10 53BP1 foci per nucleus was calculated from three independent experiments.

For the PFGE assay, subconfluent cells were irradiated with 100 Gy IR and incubated at 37°C for 24 hr. Irradiated and non-irradiated cells were washed once with PBS, trypsinized, and counted. One million cells per sample (in duplicate) were centrifuged and washed a second time with PBS. Cell pellets were resuspended in 50 µl 10 mM Tris pH 7.2, 20 mM NaCl, 50 mM EDTA and pre-warmed at 55°C for 10 min. The cell suspension was then mixed with 50 µl of 2% agarose/PBS at 55°C and solidified in plastic molds (BioRad). Agarose plugs were incubated with 1 mg/ml Proteinase K, 0.2% sodium deoxycholate, 1% N-lauroylsarcosine-sodium salt, 100 mM EDTA, pH 8.0 for 20 hr at 50°C and then washed four times for 1 hr with 20 mM Tris/HCl, 50 mM EDTA, pH 8.0. Duplicate plugs were irradiated with 600 Gy IR, and all samples were equilibrated in 0.5× TBE for 30 min. Agarose plugs were inserted into the wells of a 1% agarose gel and sealed with 1% agarose. PFGE was carried out using a CHEF-II apparatus in 0.5× TBE buffer at 6 V/cm with pulse times of 70 sec (15 hr) and 120 sec (11 hr). Following electrophoresis, the gel was stained with 0.5 µg/ml ethidium bromide in TBE for 30 min.

Supporting Information

Figure S1 C-circle assay on the ALT cell line panel. Example of dot-blot results of C-circle assay on ALT lines and non-ALT negative control (BJ/hTERT/SV40, blue). Amounts of DNA used for the assay are indicated.
(TIF)

Figure S2 Lack of ALT-mediated immortalization upon suppression of ATRX or DAXX. A, Q-RT PCR assay for the expression of hTERT mRNA in the indicated cell lines. B, C-circle assay on the indicated cell populations. JFCF-6/T.1F is a non-ALT cell line that serves as a negative control. The positive control is JFCF-6/T.1J/1-3C. C, Q-RT PCR assay for expression of DAXX mRNA in the indicated cell populations. D, Proliferation of SV40-transformed BJ fibroblasts infected with the indicated hTERT or shRNA retroviruses.
(TIF)

Figure S3 Immunoblotting for shelterin components in ALT. Immunoblots for the indicated shelterin components in whole cell extracts of the indicated cell lines.
(TIF)

Figure S4 Analysis of TERRA levels in ALT. Northern blots of total RNA from the indicated cell lines probed for TERRA with a C-strand telomeric repeat probe. The ethidium bromide staining pattern of the gel is shown with the ribosomal RNAs indicated. The bar graphs show the relative expression levels of TERRA derived from 3–5 independent experiments and standard deviations. Telomerase-positive controls, BJ/hTERT/SV40 and HeLa, are shown in blue.
(TIF)

Figure S5 Regions of recurrent amplification and deletion in 22 ALT lines. GISTIC 2.0 analysis of deletion (blue lines, left panel) and amplification (red lines, right panel) events identifies significantly recurrent peak regions (top 25 labeled by cytoband). False discovery rates (q-values; x-axis) are plotted by genomic position (y-axis) with the green line indicating the 0.25 cut-off for significance.
(TIF)

Figure S6 DDR signaling in ALT lines. Immunoblot showing phosphorylation of CHK2 before and after treatment with IR in the indicated ALT lines and the RPE/hTERT control (blue).
(TIF)

Figure S7 Example of assay for DSB repair kinetics. The graph shows the % of cells with >10 53BP1 foci scored by IF on >100 cells. The indicated cell lines were either not treated with IR, treated with 0.5 Gy and incubated for 1 hr or for 24 hr. Data from two experiments were averaged. Control telomerase-positive cell lines (blue) show disappearance of IR-induced foci. Each of the ALT lines has residual IR-induced DSBs at 24 hr.
(TIF)

Table S1 *ATRX* exons deleted in the analyzed ALT lines.
(XLSX)

Table S2 List of sequenced genes.
(XLS)

Table S3 Sequence alterations in the set of 299 genes analyzed in the ALT cell lines.
(XLSX)

Author Contributions

Conceived and designed the experiments: NP BV TdL JHJP WCH MJ NFL AKM. Performed the experiments: NP BV KK YJ CAL JB WL ST SR TdL SD JHJP BAW JR MH LM YZ EI WCH PAS CH. Analyzed the data: NP BV TdL JHJP WCH MJ NFL. Contributed reagents/materials/analysis tools: RRR. Wrote the paper: TdL JHJP WCH.

References

1. Bryan TM, Englezou A, Dalla-Pozza L, Dunham MA, Reddel RR (1997) Evidence for an alternative mechanism for maintaining telomere length in human tumors and tumor-derived cell lines. Nat Med 3: 1271–1274.
2. Dunham MA, Neumann AA, Fasching CL, Reddel RR (2000) Telomere maintenance by recombination in human cells. Nat Genet 26: 447–450.
3. Bechter OE, Shay JW, Wright WE (2004) The Frequency of Homologous Recombination in Human ALT Cells. Cell Cycle 3: 457–549.
4. Londono-Vallejo JA, Der-Sarkissian H, Cazes L, Bacchetti S, Reddel RR (2004) Alternative lengthening of telomeres is characterized by high rates of telomeric exchange. Cancer Res 64: 2324–2327.
5. Cesare AJ, Griffith JD (2004) Telomeric DNA in ALT cells is characterized by free telomeric circles and heterogeneous t-loops. Mol Cell Biol 24: 9948–9957.
6. Wang RC, Smogorzewska A, de Lange T (2004) Homologous recombination generates T-loop-sized deletions at human telomeres. Cell 119: 355–368.
7. Tokutake Y, Matsumoto T, Watanabe T, Maeda S, Tahara H, et al. (1998) Extra-chromosomal telomere repeat DNA in telomerase-negative immortalized cell lines. Biochem Biophys Res Commun 247: 765–772.
8. Henson JD, Cao Y, Huschtscha LI, Chang AC, Au AY, et al. (2009) DNA C-circles are specific and quantifiable markers of alternative-lengthening-of-telomeres activity. Nat Biotechnol 27: 1181–1185.
9. McEachern MJ, Haber JE (2005) Telomerase-independent telomere maintenance in yeast. In: de Lange T, Lundblad V, Blackburn E, editors. Telomeres. Cold Spring Harbor, New York: Cold Spring Harbor Laboratory Press. pp. 199–224.
10. Henson JD, Neumann AA, Yeager TR, Reddel RR (2002) Alternative lengthening of telomeres in mammalian cells. Oncogene 21: 598–610.
11. Yeager TR, Neumann AA, Englezou A, Huschtscha LI, Noble JR, et al. (1999) Telomerase-negative immortalized human cells contain a novel type of promyelocytic leukemia (PML) body. Cancer Res 59: 4175–4179.
12. Jiang WQ, Zhong ZH, Henson JD, Neumann AA, Chang AC, et al. (2005) Suppression of alternative lengthening of telomeres by Sp100-mediated sequestration of the MRE11/RAD50/NBS1 complex. Mol Cell Biol 25: 2708–2721.
13. Compton SA, Choi JH, Cesare AJ, Ozgur S, Griffith JD (2007) Xrcc3 and Nbs1 are required for the production of extrachromosomal telomeric circles in human alternative lengthening of telomere cells. Cancer Res 67: 1513–1519.
14. Potts PR, Yu H (2007) The SMC5/6 complex maintains telomere length in ALT cancer cells through SUMOylation of telomere-binding proteins. Nat Struct Mol Biol 14: 581–590.
15. Zeng S, Xiang T, Pandita TK, Gonzalez-Suarez I, Gonzalo S, et al. (2009) Telomere recombination requires the MUS81 endonuclease. Nat Cell Biol 11: 616–623.
16. Heaphy CM, Subhawong AP, Hong SM, Goggins MG, Montgomery EA, et al. (2011) Prevalence of the alternative lengthening of telomeres telomere maintenance mechanism in human cancer subtypes. Am J Pathol 179: 1608–1615.
17. Henson JD, Reddel RR (2010) Assaying and investigating Alternative Lengthening of Telomeres activity in human cells and cancers. FEBS Lett 584: 3800–3811.
18. Henson JD, Hannay JA, McCarthy SW, Royds JA, Yeager TR, et al. (2005) A robust assay for alternative lengthening of telomeres in tumors shows the significance of alternative lengthening of telomeres in sarcomas and astrocytomas. Clin Cancer Res 11: 217-225.
19. Sfeir A, Kabir S, van Overbeek M, Celli GB, de Lange T (2010) Loss of Rap1 induces telomere recombination in the absence of NHEJ or a DNA damage signal. Science 327: 1657–1661.
20. Kibe T, Osawa GA, Keegan CE, de Lange T (2010) Telomere protection by TPP1 Is mediated by POT1a and POT1b. Mol Cell Biol 30: 1059–1066.
21. Rai R, Zheng H, He H, Luo Y, Multani A, et al. (2010) The function of classical and alternative non-homologous end-joining pathways in the fusion of dysfunctional telomeres. EMBO J 29: 2598–2610.
22. Wang Y, Ghosh G, Hendrickson EA (2009) Ku86 represses lethal telomere deletion events in human somatic cells. Proc Natl Acad Sci U S A 106: 12430–12435.
23. Celli GB, Lazzerini Denchi E, de Lange T (2006) Ku70 stimulates fusion of dysfunctional telomeres yet protects chromosome ends from homologous recombination. Nat Cell Biol 8: 885–890.
24. Heaphy CM, de Wilde RF, Jiao Y, Klein AP, Edil BH, et al. (2011) Altered telomeres in tumors with ATRX and DAXX mutations. Science 333: 425.
25. Jiao Y, Shi C, Edil BH, de Wilde RF, Klimstra DS, et al. (2011) DAXX/ATRX, MEN1, and mTOR pathway genes are frequently altered in pancreatic neuroendocrine tumors. Science 331: 1199–1203.
26. Schwartzentruber J, Korshunov A, Liu XY, Jones DT, Pfaff E, et al. (2012) Driver mutations in histone H3.3 and chromatin remodelling genes in paediatric glioblastoma. Nature 482: 226–231.
27. Drane P, Ouararhni K, Depaux A, Shuaib M, Hamiche A (2010) The death-associated protein DAXX is a novel histone chaperone involved in the replication-independent deposition of H3.3. Genes Dev 24: 1253–1265.
28. Law MJ, Lower KM, Voon HP, Hughes JR, Garrick D, et al. (2010) ATR-X syndrome protein targets tandem repeats and influences allele-specific expression in a size-dependent manner. Cell 143: 367–378.
29. Wong LH, McGhie JD, Sim M, Anderson MA, Ahn S, et al. (2010) ATRX interacts with H3.3 in maintaining telomere structural integrity in pluripotent embryonic stem cells. Genome Res 20: 351–360.
30. Lewis PW, Elsaesser SJ, Noh KM, Stadler SC, Allis CD (2010) Daxx is an H3.3-specific histone chaperone and cooperates with ATRX in replication-independent chromatin assembly at telomeres. Proc Natl Acad Sci U S A 107: 14075–14080.
31. Goldberg AD, Banaszynski LA, Noh KM, Lewis PW, Elsaesser SJ, et al. (2010) Distinct factors control histone variant H3.3 localization at specific genomic regions. Cell 140: 678–691.
32. Azzalin CM, Reichenbach P, Khoriauli L, Giulotto E, Lingner J (2007) Telomeric repeat containing RNA and RNA surveillance factors at mammalian chromosome ends. Science 318: 798–801.
33. Baumann C, Viveiros MM, De La Fuente R (2010) Loss of maternal ATRX results in centromere instability and aneuploidy in the mammalian oocyte and pre-implantation embryo. PLoS Genet 6: e1001137. doi:10.1371/journal.pgen.1001137
34. De La Fuente R, Viveiros MM, Wigglesworth K, Eppig JJ (2004) ATRX, a member of the SNF2 family of helicase/ATPases, is required for chromosome alignment and meiotic spindle organization in metaphase II stage mouse oocytes. Dev Biol 272: 1–14.
35. Ritchie K, Seah C, Moulin J, Isaac C, Dick F, et al. (2008) Loss of ATRX leads to chromosome cohesion and congression defects. J Cell Biol 180: 315–324.
36. Ishov AM, Vladimirova OV, Maul GG (2004) Heterochromatin and ND10 are cell-cycle regulated and phosphorylation-dependent alternate nuclear sites of the transcription repressor Daxx and SWI/SNF protein ATRX. J Cell Sci 117: 3807–3820.
37. Xue Y, Gibbons R, Yan Z, Yang D, McDowell TL, et al. (2003) The ATRX syndrome protein forms a chromatin-remodeling complex with Daxx and localizes in promyelocytic leukemia nuclear bodies. Proc Natl Acad Sci U S A 100: 10635–10640.
38. Ng LJ, Cropley JE, Pickett HA, Reddel RR, Suter CM (2009) Telomerase activity is associated with an increase in DNA methylation at the proximal subtelomere and a reduction in telomeric transcription. Nucleic Acids Res 37: 1152–1159.
39. Beroukhim R, Mermel CH, Porter D, Wei G, Raychaudhuri S, et al. (2010) The landscape of somatic copy-number alteration across human cancers. Nature 463: 899–905.
40. Davoli T, Denchi EL, de Lange T (2010) Persistent telomere damage induces bypass of mitosis and tetraploidy. Cell 141: 81–93.
41. Artandi SE, Chang S, Lee SL, Alson S, Gottlieb GJ, et al. (2000) Telomere dysfunction promotes non-reciprocal translocations and epithelial cancers in mice. Nature 406: 641–645.
42. Scheel C, Schaefer KL, Jauch A, Keller M, Wai D, et al. (2001) Alternative lengthening of telomeres is associated with chromosomal instability in osteosarcomas. Oncogene 20: 3835–3844.
43. Counter CM, Avilion AA, LeFeuvre CE, Stewart NG, Greider CW, et al. (1992) Telomere shortening associated with chromosome instability is arrested in immortal cells which express telomerase activity. Embo J 11: 1921–1929.
44. Chin K, De Solorzano CO, Knowles D, Jones A, Chou W, et al. (2004) In situ analyses of genome instability in breast cancer. Nat Genet 36: 984–988.
45. Crasta K, Ganem NJ, Dagher R, Lantermann AB, Ivanova EV, et al. (2012) DNA breaks and chromosome pulverization from errors in mitosis. Nature 482: 53–58.
46. Bakou K, Stephanou G, Andrianopoulos C, Demopoulos NA (2002) Spontaneous and spindle poison-induced micronuclei and chromosome non-disjunction in cytokinesis-blocked lymphocytes from two age groups of women. Mutagenesis 17: 233–239.
47. Stracker TH, Williams BR, Deriano L, Theunissen JW, Adelman CA, et al. (2009) Artemis and nonhomologous end joining-independent influence of DNA-dependent protein kinase catalytic subunit on chromosome stability. Mol Cell Biol 29: 503–514.
48. Lu-Hesselmann J, Abend M, van Beuningen D (2004) Comparison of endogenous TP53 genomic status with clonogenicity and different modes of cell death after X irradiation. Radiat Res 161: 39–47.
49. Brown EJ, Baltimore D (2003) Essential and dispensable roles of ATR in cell cycle arrest and genome maintenance. Genes Dev 17: 615–628.
50. Kim ST, Xu B, Kastan MB (2002) Involvement of the cohesin protein, Smc1, in Atm-dependent and independent responses to DNA damage. Genes Dev 16: 560–570.
51. Abreu E, Aritonovska E, Reichenbach P, Cristofari G, Culp B, et al. (2010) TIN2-tethered TPP1 recruits human telomerase to telomeres in vivo. Mol Cell Biol 30: 2971–2982.
52. Cesare AJ, Kaul Z, Cohen SB, Napier CE, Pickett HA, et al. (2009) Spontaneous occurrence of telomeric DNA damage response in the absence of chromosome fusions. Nat Struct Mol Biol 16: 1244–1251.
53. Turner N, Tutt A, Ashworth A (2005) Targeting the DNA repair defect of BRCA tumours. Curr Opin Pharmacol 5: 388–393.
54. Bucher N, Britten CD (2008) G2 checkpoint abrogation and checkpoint kinase-1 targeting in the treatment of cancer. Br J Cancer 98: 523–528.

55. Jackson SP, Bartek J (2009) The DNA-damage response in human biology and disease. Nature 461: 1071–1078.
56. Takai KK, Hooper S, Blackwood S, Gandhi R, de Lange T (2010) In vivo stoichiometry of shelterin components. J Biol Chem 285: 1457–1467.
57. Sjoblom T, Jones S, Wood LD, Parsons DW, Lin J, et al. (2006) The consensus coding sequences of human breast and colorectal cancers. Science 314: 268–274.
58. Cancer Genome Atlas Research Network (2008) Comprehensive genomic characterization defines human glioblastoma genes and core pathways. Nature 455: 1061–1068.
59. Mermel CH, Schumacher SE, Hill B, Meyerson ML, Beroukhim R, et al. (2011) GISTIC2.0 facilitates sensitive and confident localization of the targets of focal somatic copy-number alteration in human cancers. Genome Biol 12: R41.